environments

MDPI

Systematic Review

Global Research Trends and Thematic Evolution in Rhizosphere Oxygen Environments and Microbial Communities: A Bibliometric Review from 1980 to 2026

Dekun Yu [1], Yiming Lei [1,2], Yufei Chen [1], Lingli Fan [1], Yaxin Zhang [1], Jingchun Liu [1], Haoliang Lu [1,*] and Hualong Hong [1,2,*]

[1] Key Laboratory of the Ministry of Education for Coastal and Wetland Ecosystems, Xiamen University, Xiamen 361102, China; 37520232205056@stu.xmu.edu.cn (D.Y.); 33120241152277@stu.xmu.edu.cn (Y.L.); 33120241152351@stu.xmu.edu.cn (Y.C.); 33120251152187@stu.xmu.edu.cn (L.F.); 33120261152491@stu.xmu.edu.cn (Y.Z.); liujingchun@xmu.edu.cn (J.L.)

[2] National Field Observation and Research Station (Fujian Taiwan Strait) for Marine Ecosystem, Xiamen University, Zhangzhou 363000, China

* Correspondence: luhl@xmu.edu.cn (H.L.); honghl@xmu.edu.cn (H.H.)

Abstract

Oxygen supply and consumption create heterogeneous rhizosphere environments that regulate microbial activity and biogeochemical transformations. This study combines bibliometric analysis with a synthesis of representative research to characterize the development of this field. A screened collection of 2459 Web of Science publications from 1980 to 2026 was analyzed using publication statistics, collaboration networks, author–keyword co-occurrence, and burst detection. Annual output increased overall, with an intervening period of fluctuation and renewed expansion after 2010. China, the United States, and Germany were the leading contributors. The keyword network resolved six interconnected themes encompassing symbiotic nitrogen fixation, rice-associated microbial communities and contaminants, wetland aeration and methane processes, rhizosphere nutrient and redox transformations, constructed-wetland nitrogen removal, and reactive oxygen species and root exudates. Recent bursts in microbial community and reactive oxygen species, together with work on root exudates and iron plaque, highlight growing attention to the biological regulation of rhizosphere processes. The mechanistic literature shows that roots can act as oxygen sources or sinks, and that the consequences for carbon, nitrogen, and contaminant transformations depend on substrate supply and the spatial and temporal arrangement of redox microsites. Linking oxygen imaging with isotope tracing, microbial functional experiments, and field-scale flux measurements offers a route to connect these microsite processes with ecosystem outcomes.

Keywords: bibliometrics; VOSviewer; rhizosphere microorganisms; radial oxygen loss; redox; nitrogen fixation

Check for updates

Academic Editors: Jelena Stanković Ristić, Maja Raković, Danijela Joksimović and Uroš Živković

Received: 20 September 2026
Revised: 28 October 2026
Accepted: 29 October 2026
Published: 31 October 2026

Copyright: © 2026 by the authors. Licensee MDPI, Basel, Switzerland. This article is an open access article distributed under the terms and conditions of the Creative Commons Attribution (CC BY) license.

1. Introduction

The rhizosphere is the narrow zone of soil surrounding roots that is directly influenced by root activity [1]. Plants release substantial amounts of photosynthetically derived carbon into this zone, supporting microorganisms that participate in nutrient mineralization and transformation and influence plant growth [2,3]. Root exudates sustain diverse communities of bacteria, archaea, and fungi involved in these processes [4]. The rhizosphere is therefore

an interface of intense interactions among plants, soil, and microorganisms, and a key region for understanding terrestrial ecosystem functioning.

Oxygen is one of the principal environmental factors regulating rhizosphere processes. The combined effects of root respiration, microbial oxygen consumption, and resistance to diffusion through soil produce highly heterogeneous oxygen distributions. Steep oxygen gradients and adjacent oxic and anoxic redox microsites often develop over millimeter scales, profoundly affecting microbial spatial distributions and metabolism. Along oxygen gradients at the root–soil interface, aerobic, facultatively anaerobic, and anaerobic microorganisms become spatially differentiated and perform complementary metabolic functions [5,6].

Oxygen–microorganism coupling regulates ecological and environmental processes of global significance. It influences the production and emission of N_2O and CH_4 and is an important component of greenhouse gas budgets in rice paddies and wetlands [7]. It also affects iron-plaque formation on root surfaces and the mobility and bioavailability of metals and metalloids, such as cadmium and arsenic, with implications for agricultural soil contamination and food safety [8]. In addition, it contributes to the regulation of carbon, nitrogen, and other elemental cycles. These processes are closely linked to climate change, food security, and contaminated-soil remediation, giving this field both fundamental scientific importance and practical relevance.

Research on rhizosphere oxygen–microorganism interactions is highly interdisciplinary. Relevant findings are dispersed across journals in wetland ecology, agronomy, environmental microbiology, environmental engineering, and biogeochemistry, and the field's knowledge structure and development have yet to be systematically synthesized. Narrative reviews provide detailed accounts of specific mechanisms, while bibliometric analysis can complement them by mapping publication patterns and thematic connections across the field [9].

Bibliometrics uses quantitative analysis of large publication and citation datasets to reveal knowledge structures, leading research contributors, and developmental trajectories [9]. Bibliometric approaches have increasingly been applied to soil microorganisms and microbiomes; for example, Sun et al. mapped rhizosphere microorganism research for 2012–2021 [10], and Wang et al. analyzed the rhizosphere microbiota of wetland plants using CiteSpace [11]. However, the redox dimension that links plants and microorganisms has not been synthesized at the bibliometric level. Further integrated analysis is therefore needed to clarify knowledge connections and research evolution at the intersection of rhizosphere oxygen and microorganisms.

This study uses bibliometric methods to analyze publications on rhizosphere oxygen–microorganism interactions in terms of publication trends, country/region and author collaborations, journal and subject distributions, and keyword co-occurrence and bursts. The objectives are to (1) identify major collaboration hubs; (2) characterize research themes and their evolution; and (3) draw on representative studies to discuss research frontiers and future directions, focusing on advances in rhizosphere oxygen imaging, microfluidics, and stable isotope tracing, together with themes such as microbiome research and biochar-mediated regulation.

2. Materials and Methods

2.1. Data Source and Search Strategy

Bibliographic records were retrieved from the Web of Science Core Collection (Clarivate) on 17 September 2026 and exported with cited references. The database provides the bibliographic, affiliation, keyword, and cited-reference fields required for the analyses. The complete query and retrieval information are provided in Supplementary Methods S1.

The search intersected three concept sets: the root–soil interface, oxygen or redox conditions, and microorganisms. The interface set included rhizosphere, rhizoplane, root-associated environments, and root nodules. The oxygen/redox set included direct descriptors such as oxygen, hypoxia, and radial oxygen loss, together with related indicators such as electron acceptors and iron species. The microbial set covered microorganisms and functional groups involved in nitrogen, carbon, and sulfur transformations. The search retrieved 5578 records. Bibliographic eligibility and content-based scope assessment were applied before analysis (see Section 2.2).

2.2. Screening, Eligibility, and Thematic Scope Assessment

Record identification, eligibility assessment, and exclusions are reported using the applicable elements of PRISMA 2020 [12] (Figure S1; Table S1). Screening concerned bibliographic eligibility and thematic relevance based on titles, abstracts, and author keywords. Effect sizes were not pooled, and no formal risk-of-bias assessment was performed. The record-level screening ledger is available from the corresponding author upon reasonable request.

Sequential screening removed 2 duplicates, 76 records outside SCIE or ESCI, 25 records other than articles or reviews, 27 non-English records, and 3 retracted records, leaving 5445 records for thematic assessment. Duplicates were identified using the DOI, title, and publication details. The final analytical collection contained 2459 records dated 1980–2026, of which 214 were dated 2026. All included records contributed to the descriptive statistics and network analyses. Trend modeling and burst detection used the 2245 records from the complete calendar years 1980–2025 (Table S2). Author keywords (DE), rather than keywords plus (ID), were used in the primary keyword analyses; their availability by publication period is reported in Table S3, and a comparison using the union of DE and ID terms is reported in Table S4.

Thematic relevance was first assessed with Intern-Decision-4B using titles, publication years, sources, author keywords, and abstracts. Predicted probabilities were converted into inclusion decisions using a Bayesian prior-adjustment rule with an ambiguity band. This step retained 2071 of the 5445 candidate records. Model providers, access dates, input specifications, and decision rules are reported in Supplementary Methods S9.

A second classifier, DeepSeek-V4.1-Flash, independently applied the same thematic screening criteria without access to the first classifier's decisions. Level 1 denoted direct measurement or manipulation of oxygen/redox conditions; level 2 denoted an explicit mechanistic role for oxygen or redox; level 3 denoted no substantive connection or only a routine growth-condition descriptor. Levels 1 and 2 were included. The record-level cross-tabulation confirmed that each classifier retained 2071 records, but their selections differed: 1683 were retained by both, and each retained 388 records that the other excluded. Their union formed the final sample of 2459 records, leaving 2986 thematic exclusions. The intersection and first-classifier samples were retained as alternative inclusion specifications (Table S5).

A decade-stratified random sample of 120 candidate records was assessed by one reviewer using the titles, abstracts, and author keywords, with classifier decisions concealed. The reviewer applied the same three-level scope rubric, treating levels 1 and 2 as relevant. The final union-rule decisions were compared with these human judgements to calculate precision, recall, and Cohen's κ. Wilson 95% confidence intervals were calculated for precision and recall. Here, κ measures the agreement between screening decisions and the single-reviewer reference (Table S6). Because the same 120-record sample was used to estimate the prior, this audit is an internal check of the screening rule rather than an independent validation.

Scope checks examined three features of the collection: the overlap between the two classifiers, the prevalence of direct oxygen/redox terminology within the included records, and the presence of genome announcements or taxonomic descriptions. The latter were identified using title expressions such as sp. nov., gen. nov., draft genome, and genome announcement, together with source and document-type information. Nine included records were flagged by this rule (0.37%); the corresponding figure in the 5445-record candidate pool was 687 (12.62%). These checks describe the sample composition and complement the single-reviewer audit (Tables S5, S7 and S8).

2.3. Analytical Methods and Tools

Bibliographic records were parsed with the VOSviewer Web of Science reader and Python 3.12. Country names and author keywords were harmonized using archived thesauri; the keyword mappings are provided in Table S9. Author names were standardized for case but were not disambiguated across initials and full names. VOSviewer 1.6.21 was used for network layout, clustering, and visualization, with association-strength normalization and full counting [13,14]. Frequencies of cited-reference strings are summarized in Table S10. Country and author maps show the largest connected components among entities with at least three publications; the keyword map includes author keywords occurring in at least ten publications. Links represent at least one shared publication for countries and authors, or at least one co-occurrence for keywords; degree-one nodes were retained. Node size indicates the publication count for countries and authors as well as the occurrence count for keywords; link thickness indicates the corresponding collaboration or co-occurrence frequency; and color indicates cluster or average publication year. Network parameters and counts are reported in Table S11. Country publication totals count each country once per publication; fractional counts assign 1/k to each of the k countries on a paper. Degree, total link strength, and unweighted normalized betweenness were calculated on the complete country network with NetworkX 3.7 (Table S12). Alternative thresholds are reported in Table S13.

Annual publication counts were analyzed for 1980–2025. Linear, exponential, quadratic, logistic, and Gompertz models were fitted to annual counts by least squares and compared using AIC and BIC. Residual diagnostics were used to assess the adequacy of a single growth curve (Table S14; Figure S2). Segmented descriptions of the log annual series were used to characterize changes in the trajectory (Table S15); the stage labels describe publication patterns.

Keyword bursts were identified using a two-state model based on Kleinberg's framework [15], with state multiplier $s = 2$ and upward-transition penalty $\gamma \ln(T)$, where $\gamma = 1$ and $T = 46$ annual intervals (1980–2025). Candidate keywords occurred in at least 20 publications during this period. Each year's denominator was the number of publications with available author keywords. The baseline probability was the keyword's overall frequency among these records, and the high-state probability was twice the baseline, capped below one. Burst strength was the summed log-likelihood gain of the high state over the baseline during each detected interval. A calculation using all annual publications as denominators was retained for comparison (Table S16).

2.4. The Representative Literature and Evidence Types

Representative studies for the discussion were selected with reference to the six keyword clusters, the temporal distribution of research, citation visibility, and relevance to the mechanisms under discussion. Recent studies with direct oxygen/redox observations or interventions were considered alongside foundational work on the same processes. Citation counts informed selection but were not treated as measures of methodological quality. The

selected studies were read in full where available or assessed from their titles and abstracts, and their systems, evidence types, and thematic roles are summarized in Table S17. The bibliometric analyses characterize the literature, whereas the mechanistic synthesis draws on experimental findings in these individual studies.

3. Results

3.1. Publication Output

Annual output showed an overall increase with a pronounced intermediate plateau (Figure 1a; Table S18). The early expansion from the 1980s to the early 1990s was followed by fluctuating output of roughly 30–50 papers per year through 2010. Publication activity increased again after 2010, reaching 161 papers in 2025; additionally, the 627 papers published in 2021–2025 accounted for 27.9% of the complete-year collection. These patterns support a descriptive distinction between early expansion, an intermediate period of fluctuation, and recent expansion. The exponential model had the lowest AIC and BIC among the five fitted specifications, but residual autocorrelation indicates that a single growth curve does not capture the intervening fluctuations (Table S14). The 214 records dated 2026 are shown separately as an incomplete-year count and were excluded from trend estimation.

The 2335 records with parsable country information involved 94 countries or regions (Table S19). China, the United States, and Germany contributed the largest numbers of publications (Table 1; Figure 1b), while France, the United Kingdom, Australia, and Japan also formed substantial parts of the collection. Papers involving China or the United States comprised 48.8% of the dataset after their joint publications were counted once. This geographic concentration coexists with a broader international distribution across both plant-science and environmental research settings.

Table 1. Top 10 countries/regions by publication count, with their share of the dataset and average publication year.

Rank	Country/Region	Publications	Share (%)	Mean Year
1	China	790	32.1	2020.9
2	United States	456	18.5	2009.4
3	Germany	240	9.8	2011.3
4	France	157	6.4	2008.8
5	United Kingdom	138	5.6	2008.5
6	Australia	134	5.4	2012.5
7	India	118	4.8	2016.7
8	Japan	117	4.8	2012.9
9	Spain	107	4.4	2012.2
10	Denmark	90	3.7	2011.0

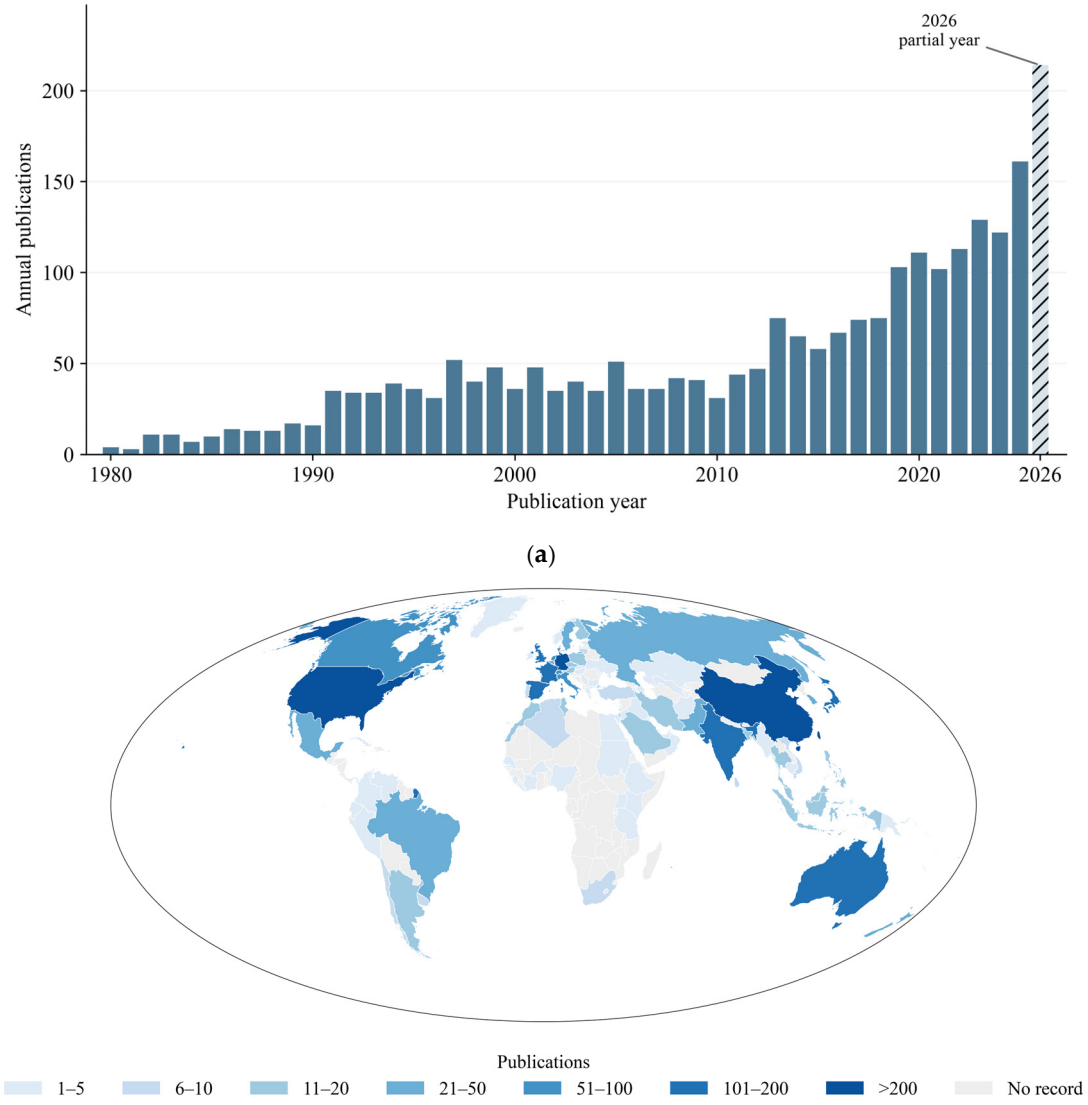


Figure 1. Publication output and geographic distribution: (**a**) Annual publication counts, 1980–2026; the hatched 2026 bar represents the incomplete year at the search date and is excluded from trend modeling. (**b**) Country/region publication counts based on author affiliations and full counting.

3.2. Collaboration Patterns by Country and Region

The country collaboration map contained 64 countries and 402 links (Figure 2a). China–United States and China–Germany collaborations were the strongest pairs, with 46 joint publications each, followed by China–Australia with 36. Their shared research extended across several substantive problems. China–Germany papers included rice-root iron plaque, carbon retention, and phosphorus mobilization, while China–United States collaborations included redox-mediated root-microbiome assembly, nitrogen transformations, and contaminant degradation in planted sediments. China–Australia papers addressed rice-rhizosphere iron and arsenic processes as well as biochar-related changes in nutrient acquisition. These collaborations therefore connect plant physiology and microbial mechanisms with nutrient management and pollutant behavior.

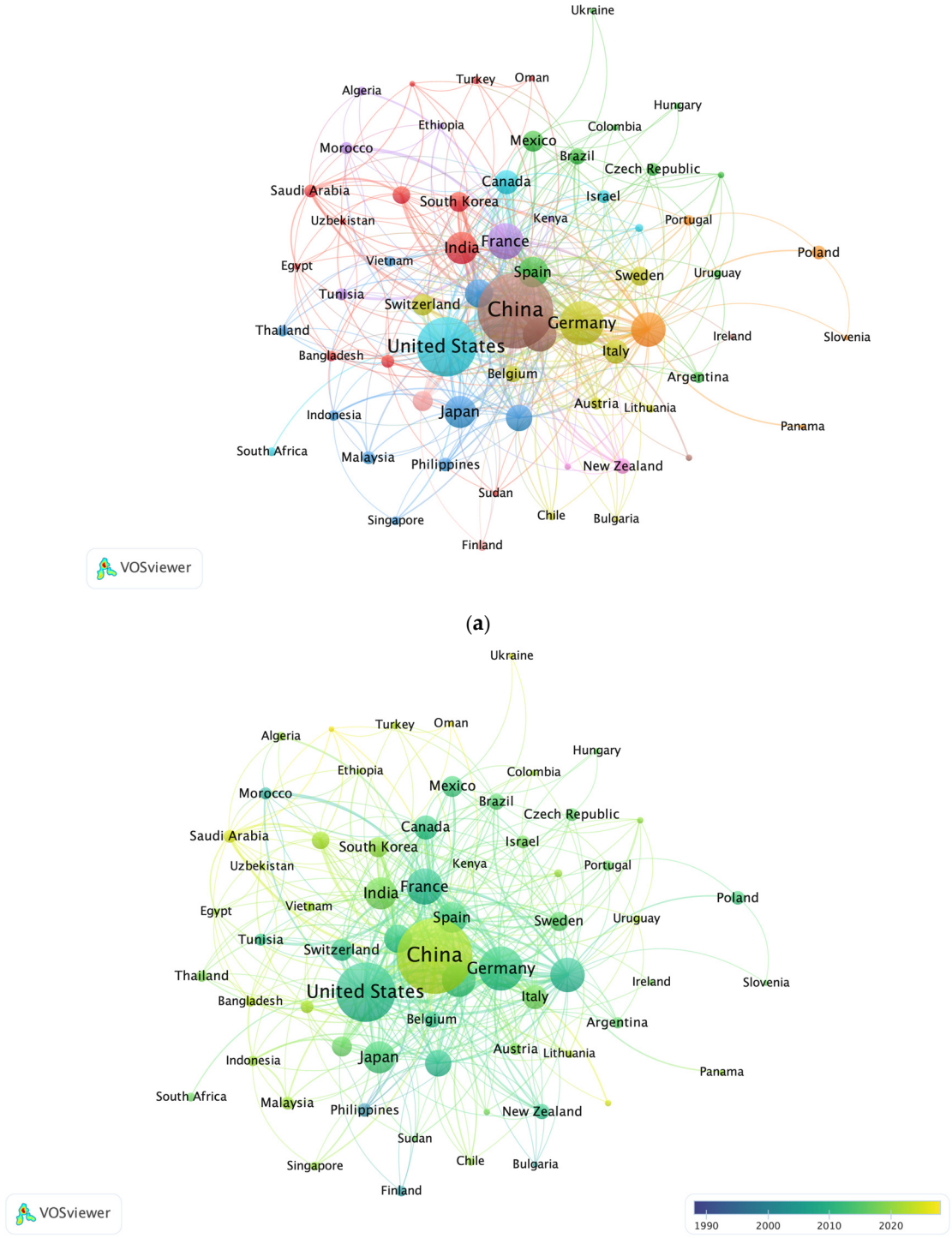


Figure 2. Country/region collaboration network generated in VOSviewer: (**a**) Cluster view. (**b**) Overlay of the average publication year on the same network (blue, earlier; yellow, more recent). Node size denotes publication count; link thickness denotes collaboration strength; node color denotes cluster (**a**) or average publication year (**b**).

The overlay map distinguishes earlier and more recent publication portfolios (Figure 2b). The mean publication year was 2009.4 for the United States and 2020.9 for China. This difference reflects the composition of the retrieved literature: early United States papers included nodule oxygen regulation, nitrogen fixation, and wetland root–sediment transformations, whereas 672 of China's 790 records were published during 2016–2026 and included rice

microbiomes, iron plaque, root exudates, and constructed-wetland processes. China had the highest degree and total link strength in the complete country network; Germany's total link strength exceeded that of the United States, despite its smaller publication count. China, the United States, and Germany remained the three leading contributors under fractional counting (Table S12).

3.3. Author Collaboration and Core Research Teams

The dataset contained 9703 distinct author-name strings, of which 550 occurred in at least three publications. The leading organizations are listed in Table S20. The largest connected component contained 272 authors and 772 links (Figure 3). Across the full collection, Minchin F.R., Drevon J.J., and Conrad R. had 19, 18, and 17 publications, respectively (Table S21). Their papers illustrate sustained contributions to nodule oxygen regulation, nitrogen fixation, and anaerobic microbial processes. These overall publication rankings differ from the membership of the displayed connected component, which captures a subset of the collaboration structure. Initial-based and full-name variants were not merged without evidence about identity.

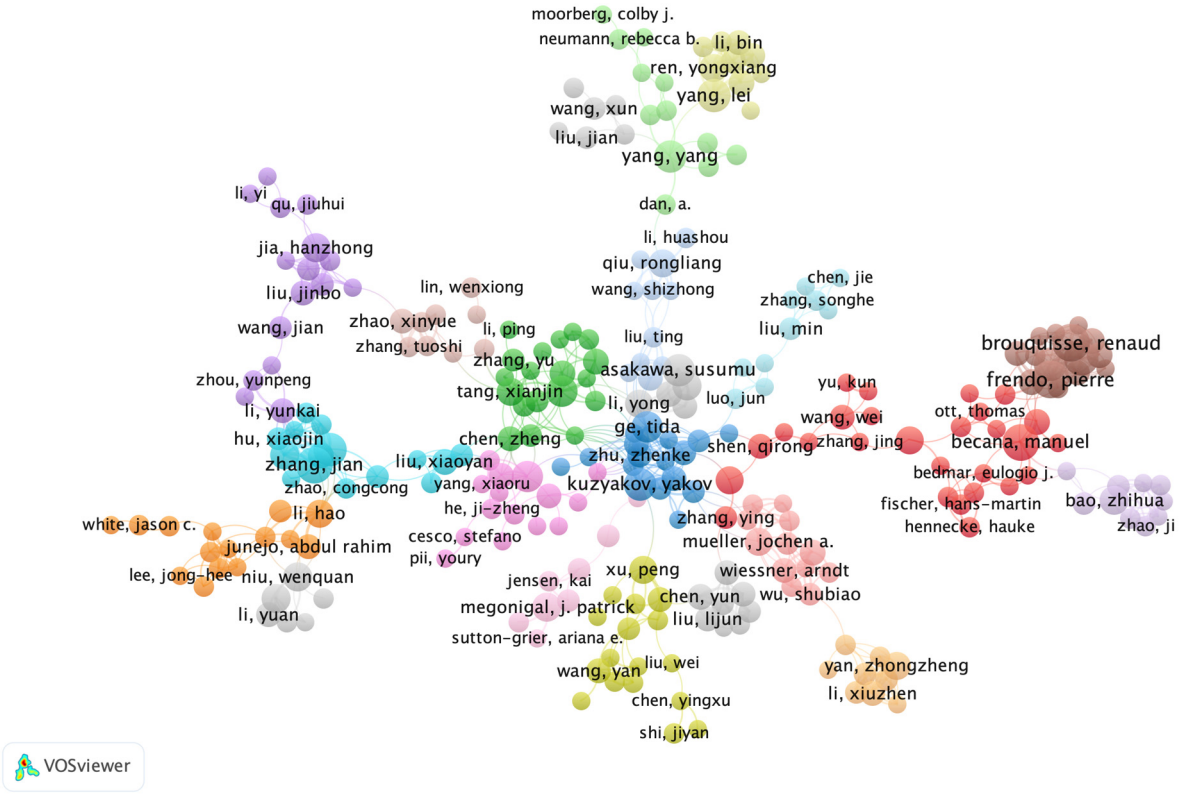


Figure 3. Author collaboration network generated in VOSviewer. Authors with at least three publications and links representing at least one shared publication were eligible; the largest connected component contains 272 nodes and 772 links. Node size denotes publication count, color denotes cluster, and line thickness denotes collaboration strength.

Within the displayed component, the group involving Brouquisse Renaud, Frendo Pierre, and Boscari Alexandre addressed nitric oxide, redox regulation, and legume symbiosis. The Kuzyakov Yakov–Ge Tida group linked rice-root carbon inputs with iron reduction, phosphorus availability, and iron-plaque carbon retention. A further group involving Zhang Jian, Xie Huijun, and Hu Zhen focused on planted treatment systems and pollutant removal. These groups connect different experimental scales: physiological regulation within root

symbioses, microbial transformations in the rhizosphere, and treatment performance in constructed wetlands.

3.4. Source Journals and Subject Distribution

The journal and subject distributions place the literature at the interface of plant function, soil microbial processes, and environmental applications (Figure 4; Table S22). *Plant and Soil* contributed the most papers (105), followed by *Soil Biology & Biochemistry* (77) and *Science of the Total Environment* (60). The presence of *Applied and Environmental Microbiology* and *Journal of Experimental Botany* alongside *Ecological Engineering* reflects both organism-level investigations and research on engineered plant–microbe systems. Environmental Sciences & Ecology, Plant Sciences, and Agriculture were the most frequent WoS research areas (Table S23); Microbiology and Engineering added complementary perspectives. Research-area assignments overlap, so these categories represent disciplinary connections rather than mutually exclusive divisions of the dataset. Genome-announcement and taxonomic-description records accounted for 9 of the 2459 included records (0.37%; Table S8).

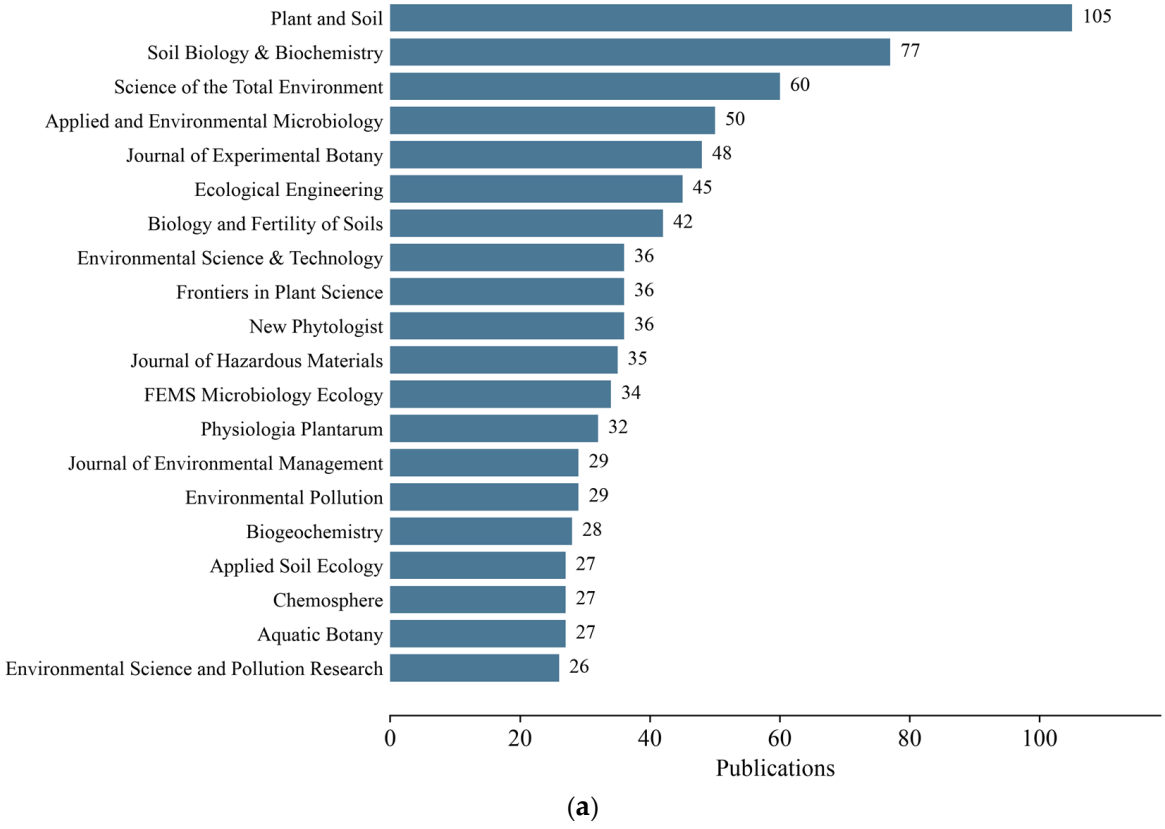


Figure 4. *Cont.*

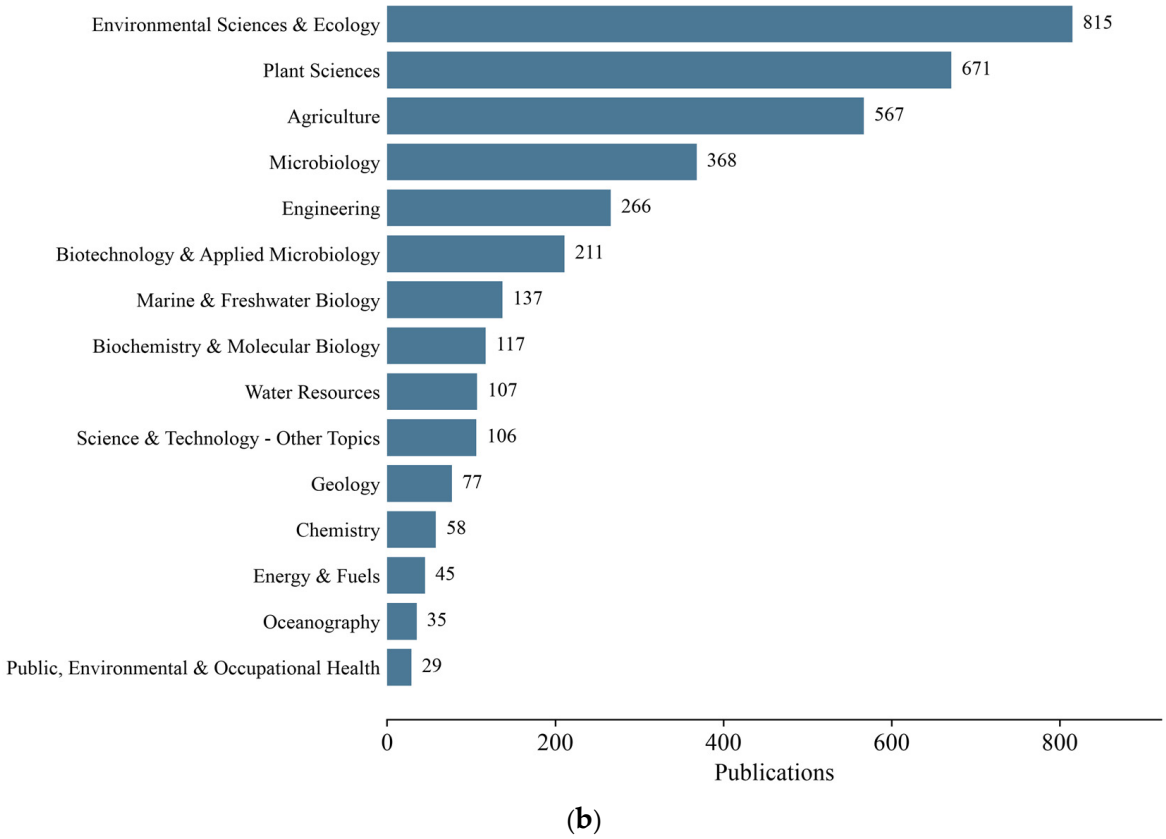
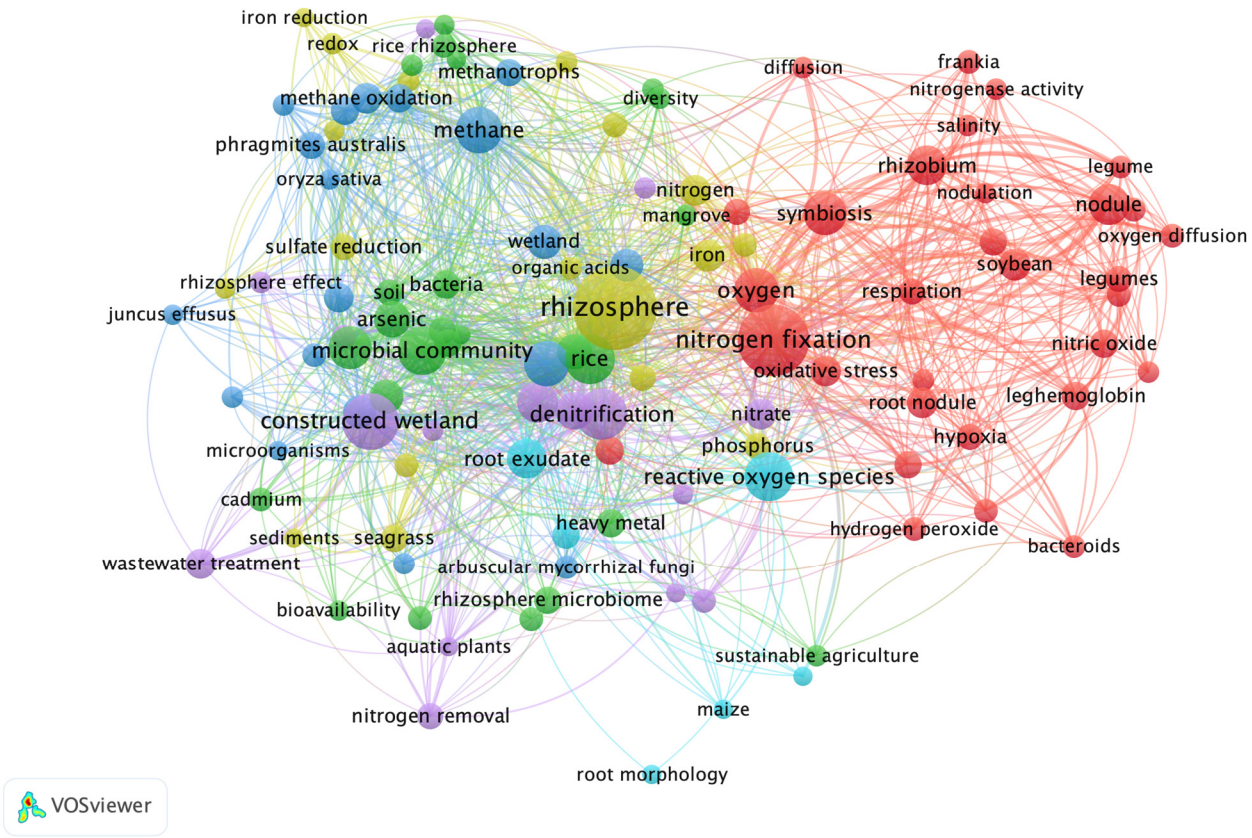


Figure 4. Publication outlets and disciplinary composition: (**a**) Twenty leading source journals. (**b**) Fifteen leading Web of Science research areas. A publication may be assigned to more than one research area.

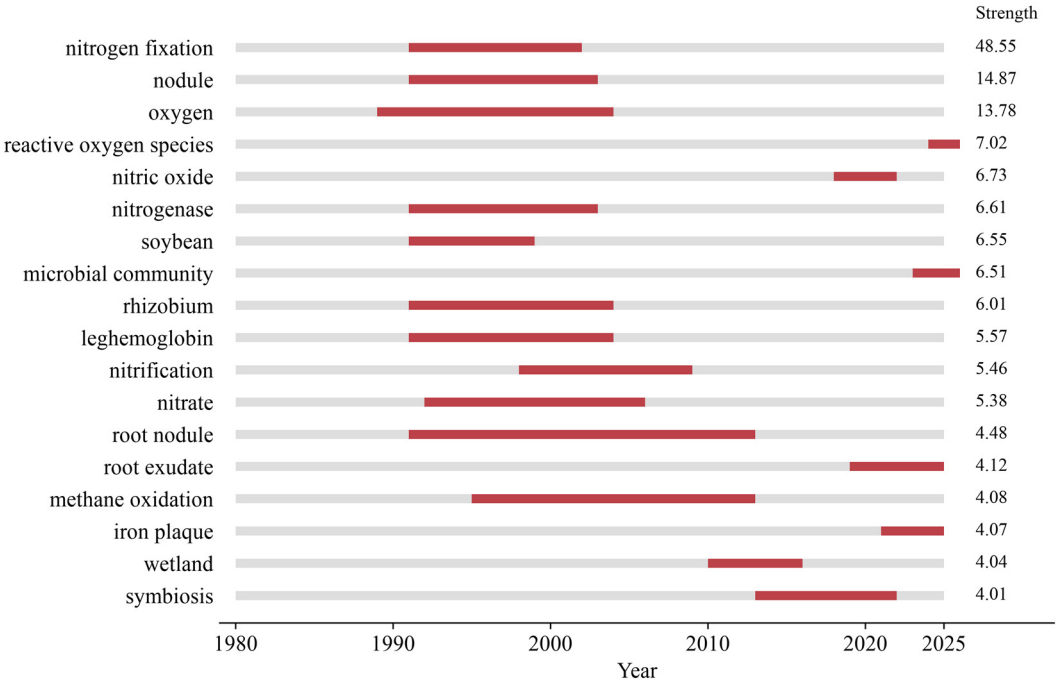
3.5. Keyword Hotspots and Research Frontiers

The author–keyword network contained 115 terms and 1197 links (Table S11), distributed across six clusters (Figure 5a; Table 2). Symbiotic nitrogen fixation formed the largest cluster, linking oxygen, nodules, rhizobium, and respiratory or oxidative regulation. A rice-associated cluster combined microbial communities, iron plaque, and contaminant-related terms, while a wetland cluster linked radial oxygen loss and aerenchyma with methane production, oxidation, and emissions. A broader rhizosphere cluster connected iron, nitrogen, sulfur, and nutrient transformations across root–sediment systems. Constructed wetlands, nitrification, and denitrification formed a treatment-oriented cluster, and reactive oxygen species and root exudates formed a smaller cluster concerned with plant–microbe regulation. These divisions distinguish research settings and processes without implying that their mechanisms are isolated from one another.

Burst analysis identified 18 keyword intervals (Figure 5b; Table 3). Nitrogen fixation showed the strongest burst during 1991–2001, accompanied by nodule, oxygen, and nitrogenase. Nitrification and methane oxidation were prominent in subsequent intervals, whereas nitric oxide, root exudate, and iron plaque became active later. Microbial community (2023–2025) and reactive oxygen species (2024–2025) remained in a burst state at the end of the complete-year observation window. The sequence indicates continuing interest in oxygen-sensitive metabolism alongside increasing attention to community regulation and the chemical interactions surrounding roots.



(**a**)



(**b**)

Figure 5. Author–keyword structure and temporal activity: (**a**) VOSviewer co-occurrence map of terms appearing in at least ten publications, with links representing at least one co-occurrence—115 nodes, 1197 links, and six clusters. Color denotes cluster. (**b**) Eighteen burst intervals identified for 1980–2025; red segments indicate the high-frequency state. Annual denominators include only publications with available author keywords.

Table 2. Six author–keyword clusters and their representative themes. Cluster labels summarize the displayed terms and are interpretive descriptors.

Cluster	Theme	Terms	Representative Keywords
1	Symbiotic nitrogen fixation and oxygen regulation	31	nitrogen fixation; oxygen; symbiosis; nodule; rhizobium
2	Rice-associated communities and contaminants	25	rice; microbial community; paddy soil; arsenic; iron plaque
3	Wetland aeration and methane processes	19	methane; radial oxygen loss; wetland; aerenchyma; methane oxidation
4	Rhizosphere nutrients and redox transformations	18	rhizosphere; iron; nitrogen; seagrass; sulfate reduction
5	Constructed-wetland nitrogen transformations	16	constructed wetland; denitrification; nitrification; redox potential
6	Reactive oxygen species and root exudates	6	reactive oxygen species; root exudate; plant growth promoting rhizobacteria

Table 3. Keyword burst intervals, ranked by strength, for 1980–2025.

Keyword	Begin	End	Strength
nitrogen fixation	1991	2001	48.55
nodule	1991	2002	14.87
oxygen	1989	2003	13.78
reactive oxygen species	2024	2025	7.02
nitric oxide	2018	2021	6.73
nitrogenase	1991	2002	6.61
soybean	1991	1998	6.55
microbial community	2023	2025	6.51
rhizobium	1991	2003	6.01
leghemoglobin	1991	2003	5.57
nitrification	1998	2008	5.46
nitrate	1992	2005	5.38
root nodule	1991	2012	4.48
root exudate	2019	2024	4.12
methane oxidation	1995	2012	4.08
iron plaque	2021	2024	4.07
wetland	2010	2015	4.04
symbiosis	2013	2021	4.01

Author keywords were available for 1963 records (79.8%). Coverage rose from 4 of 119 records in 1980–1990 to 583 of 627 in 2021–2025 (Table S3). Early burst intervals therefore describe the terminology in the keyword-bearing portion of the literature. Using the same records as annual denominators avoids treating missing keywords as observed absences of individual research topics.

3.6. Topical Scope Assessment and Sensitivity Analyses

Of the 5445 records entering thematic assessment, 2459 were included and 2986 were excluded. The classifiers agreed on inclusion of 1683 records; the 776 records included by only one classifier accounted for 31.6% of the final collection (Table S5). Within the final sample, 2090 records (85.0%) contained direct oxygen/redox terminology, and 156 (6.3%) lacked these direct terms but contained environmental descriptors (Table S7). The latter count is a vocabulary-based diagnostic. Nine records were flagged as taxonomic descriptions or genome announcements (Table S8). In the 120-record audit, 39 of 46 included records were judged as relevant (precision: 84.8%; 95% CI: 71.8–92.4%), and 39 of 61 manually relevant records were retained (recall: 63.9%; 95% CI: 51.4–74.8%). Agreement between the final screening decisions and the reviewer was 75.8%, with $\kappa = 0.519$ (Table S6).

4. Discussion

The six keyword clusters bring together research on symbiotic oxygen regulation, wetland aeration, rhizosphere communities, nutrient transformations, and contaminant behavior. The burst sequence places early emphasis on nitrogen fixation alongside more recent attention to reactive oxygen species, root exudates, and microbial communities. The methods used in this collection of literature include neighbor-joining reconstruction of phylogenetic trees from distance data [16], bootstrap resampling to assess support for inferred branches [17], and QIIME for analyzing high-throughput community sequencing data [18], while community-assembly studies connect these differences with plant selection and substrate use [3,19,20]. The following synthesis develops these links through plant–soil feedback, the electron-acceptor cascade from oxygen and nitrate through manganese and iron oxides to sulfate and carbon dioxide, and the contaminant and application domains in which these interfaces operate, drawing on the evidence types summarized in Table S17.

Oxygen supply and consumption link plant traits with microbial metabolism, but their balance differs among root systems. Root aeration, respiration, substrate supply, and the persistence of redox interfaces determine which processes can occur together or in succession. This provides a process-based way to compare the keyword themes while retaining the differences among flooded soils, wetlands, aerated rhizospheres, and legume nodules.

4.1. Plant–Soil Feedback Driven by Plant–Microbe Interactions

Recent themes, such as the rhizosphere microbiome and plant–microbe interactions, broaden the perspective from microbial responses to environmental conditions to the joint modification of those conditions by plants and microorganisms. Plants alter colonization conditions through root architecture, oxygen supply, and exudation, while microbial substrate preferences, oxygen consumption, and signaling affect plants and their surrounding environment [3,20–22]. Changes in root exudate chemistry during plant development align with microbial substrate-use traits, providing a metabolic explanation for community assembly [20]. In the context of oxygen dynamics, plant carbon supply both selects microbial communities and fuels microbial oxygen consumption. Carbon and oxygen supply should therefore be examined as interrelated plant traits [23]. The resulting feedback framework—from plant traits and internal aeration through root respiration and exudate-driven community assembly to stress alleviation and soil legacy—is summarized in Figure 6.

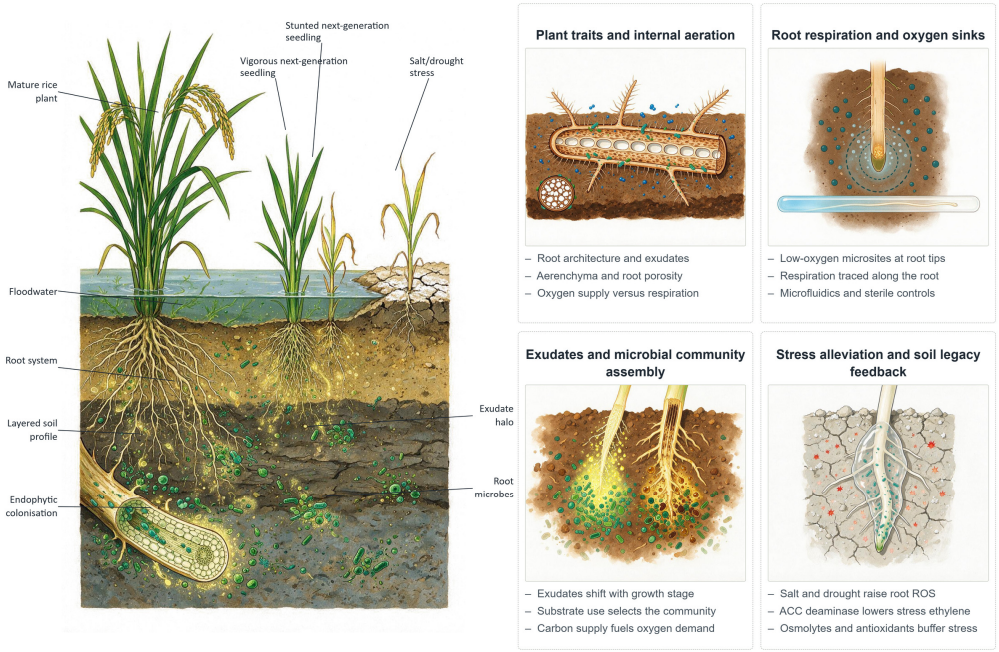


Figure 6. Plant–soil feedback linking plant oxygen supply, root respiration, exudate-mediated microbial community assembly, stress responses, and soil legacy. The left-hand soil profile and the four process panels summarize complementary mechanisms. The figure was generated with the assistance of AI tools (TraeWork v0.1.69 Design mode for the figure design and layout, DeepSeek-V4.1-Flash for drafting, and Seedream 5.0 for image generation). The authors have verified the figure's content and take full responsibility for it.

These interactions can also influence internal plant aeration structures. Inoculation of rice with the endophytic fungus *Phomopsis liquidambari* promoted root aerenchyma formation and mineral nutrient uptake [24]. Experiments combining fungal inoculation with hormonal interventions implicated auxin and ethylene signaling in aerenchyma formation [25]. In wetland plants, root porosity and radial oxygen loss were associated with rhizosphere redox conditions and pollutant removal [26]. Microbial effects thus extend from nutrient transformations outside roots to regulation of oxygen transport pathways within roots. This is consistent with evidence that root oxygen supply influences nitrification and microbial distributions on root surfaces [6,27,28]. Together, these findings support a view of plant–microbe feedback as bidirectional regulation among traits, environmental conditions, and functions: plants modify the oxygen environment experienced by microorganisms, whereas microorganisms alter plant oxygen-supply capacity through physiological processes.

Oxygen consumption by plants is also integral to this relationship. Real-time microfluidic imaging of wheat roots showed that low-oxygen microsites could form around growing root tips even under sterile conditions, indicating that root respiration alone can substantially alter local oxygen distributions. Interactions between inoculation and light–dark cycles also contributed to oxygen dynamics [29]. This observation is compatible with radial oxygen loss from wetland plants: the two phenomena reflect differences in the balance between oxygen supply and consumption across plant species and environmental conditions. The effects of plant aeration traits also depend on flooding depth and duration [30]. Roots can therefore act as either oxygen sources or oxygen sinks in their surroundings. Consequently, in flooding-stress research, the effects of beneficial microorganisms, pathogen infection, and plant tolerance should be interpreted in relation to host physiology and oxygen dynamics. The combined effects of flooding on microbial colonization and host defense are a key link between abiotic stress and plant health [31].

When plant-shaped microbial communities continue to affect subsequent plants, these interactions extend into plant–soil feedback. Microbial inoculation experiments using soils under long-term rice cultivation showed reduced seedling vigor in a common growth substrate with sterilized-inoculum controls, while inocula from some fallow soils partially restored vigor [32]. These findings indicate that cultivation history can leave a biological legacy through soil microorganisms that affects subsequent growth. Rhizosphere oxygen research can build on this insight by examining how oxygen-supply traits and water management modify such legacies. Combining soil conditioning with subsequent planting, and linking microbial inoculation, oxygen manipulation, and plant performance over time, would help resolve how immediate physiological interactions accumulate into feedback across growth stages.

Plant–microbe feedback also operates through oxidative signaling and growth responses under stress. Salinity and drought can increase reactive oxygen species and disturb hormonal balance in roots; associated bacteria and mycorrhizal fungi can modify these responses through ACC deaminase activity, antioxidant regulation, osmolytes, and extracellular polymers [33]. The cluster linking reactive oxygen species with root exudates is consistent with attention to this chemical dimension of plant–microbe interactions [34]. Reactive oxygen species are distinct from molecular oxygen availability: their production and scavenging regulate cellular responses, whereas external oxygen supply constrains respiration and redox conditions [35,36]. Connecting these two scales requires direct physiological and environmental measurements. Microbial partners also act on the plant side of this feedback. The proposed rhizophagy cycle links root-associated oxidative activity to nutrient acquisition from microbial partners [37]. Mycorrhizal symbiosis can delay drought-induced nodule senescence and sustain nitrogen fixation [38], and mycorrhization protects roots against heavy-metal-induced oxidative stress [39].

4.2. Redox Processes Across the Electron-Acceptor Cascade

4.2.1. The Electron-Acceptor Cascade: An Overview

Oxygen gradients generated jointly by plant oxygen supply, root respiration, and microbial oxygen consumption create distinct reaction microsites for elemental transformations [40]. The role of rhizosphere oxygen in biogeochemical cycling is first expressed through the spatial differentiation of processes. Flooding restricts gas diffusion through soil, whereas aerenchyma transports oxygen belowground in rice and many wetland plants [41]. Radial oxygen loss then creates localized oxidized zones within reduced soil [42–44]. Variation in the permeability among root regions, root age, and respiratory demand determines where oxygen is supplied, while oxygen consumption by soil constituents and microorganisms influences the extent of these zones [5,7,45,46]. The intersection of oxygen, available organic carbon, and different electron acceptors allows aerobic oxidation and anaerobic reduction to occur in neighboring locations or at different times, providing the basis for connections among nitrogen, carbon, iron, and sulfur processes [47–52]. Anoxic soil microsites can also alter organic carbon decomposition by changing microbial respiratory pathways and energy yields, indicating that carbon retention is regulated by both oxygen supply and mineral association [53]. The discussion below follows the electron-acceptor sequence from oxygen and nitrate through manganese and iron oxides to sulfate and carbon dioxide, and examines its connections to carbon, nitrogen, sulfur, and metal transformations [40,52]. Iron and manganese are treated separately because their oxides are the most abundant redox-active solids in these soils and act as a hub that buffers redox potential and couples carbon, nitrogen, phosphorus, and trace-metal cycling [54,55] (Figure 7a,b).

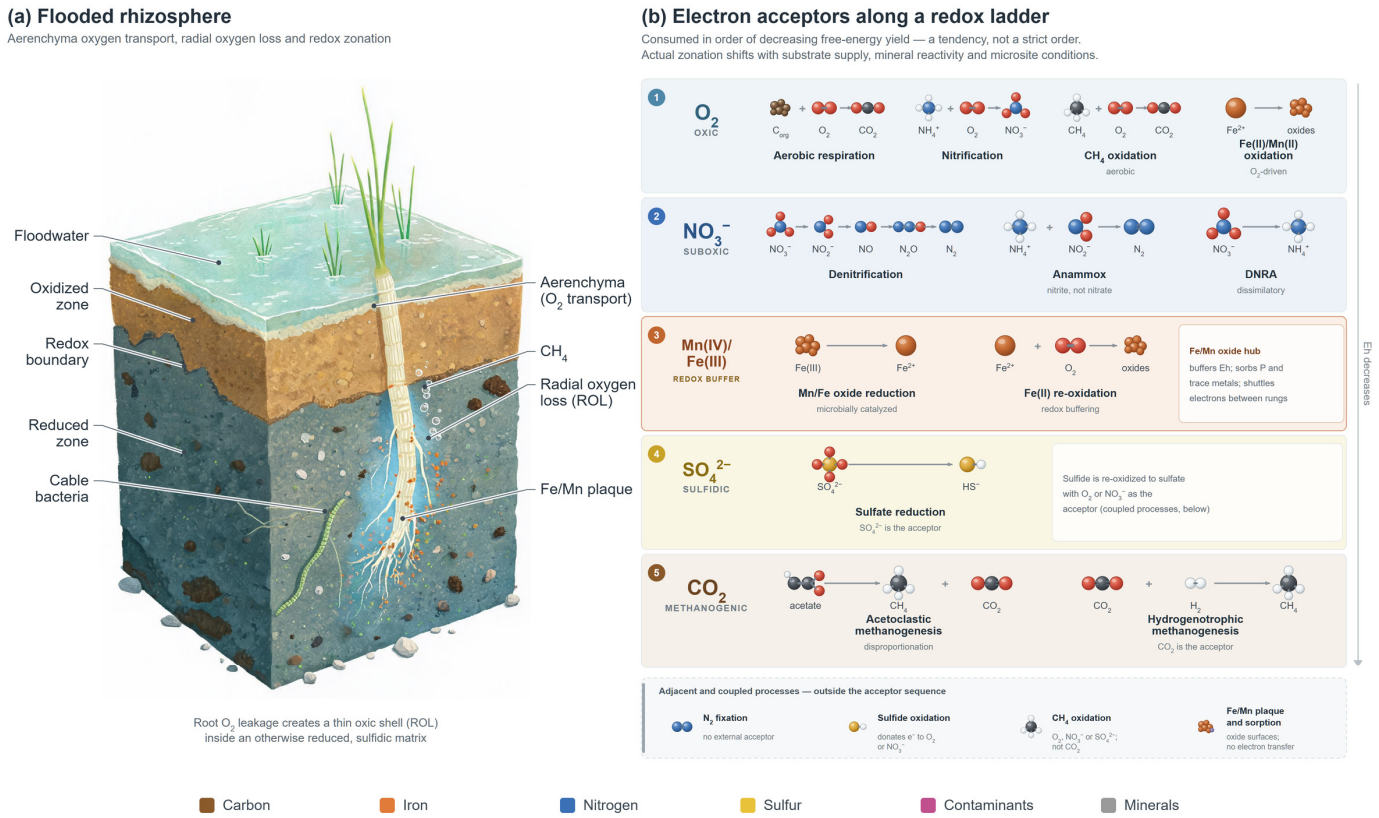


Figure 7. Redox processes in the flooded rhizosphere: (**a**) Aerenchyma-mediated oxygen transport, radial oxygen loss, redox zonation, and root-surface Fe/Mn plaque. (**b**) Processes associated with O_2, NO_3^-, Mn(IV)/Fe(III), SO_4^{2-}, and CO_2 along a redox ladder. The sequence represents a general tendency rather than a strict order; local conditions and substrate availability influence the zonation. Anammox uses nitrite rather than nitrate. CO_2 is the electron acceptor in hydrogenotrophic methanogenesis, whereas acetoclastic methanogenesis is shown as acetate disproportionation. The lower panel separates adjacent or coupled processes—including N_2 fixation, sulfide oxidation, CH_4 oxidation, and plaque-associated sorption—from the acceptor sequence. The Fe/Mn oxide hub represents redox buffering, sorption, and coupling among processes. The figure was generated with the assistance of AI tools (TraeWork v0.1.69 Design mode for the figure design and layout, DeepSeek-V4.1-Flash for drafting, and Seedream 5.0 for image generation). The authors have verified the figure's content and take full responsibility for it.

4.2.2. Nitrogen Transformations Across Redox Zones

Research on nitrogen transformations illustrates a progression from the effects of root oxygen supply to functional differentiation among microsites. Early seasonal comparisons between root zones and unvegetated sediments connected nitrifier abundance with potential nitrification and denitrification activities. Reoxygenation following anoxic incubation further showed that nitrifying communities from habitats with persistent oxygen fluctuations could retain activity and rapidly resume nitrification [56]. Subsequent comparisons of rice cultivars related differences in root porosity and radial oxygen loss to measured oxygen profiles, nitrification activity, and nitrogen accumulation [6]. Vertical observations in constructed wetlands associated higher oxygen levels in upper layers with greater ammonium removal, and lower oxygen levels at depth were associated with greater total nitrogen removal [57–59]. Together, these findings indicate that rhizosphere nitrogen transformations depend on substrate exchange between oxygenated and low-oxygen zones [60]. The former produce nitrate, while the latter use nitrate and organic carbon in reduction processes; plant uptake and microbial utilization jointly determine nitrogen fate. Nutrient retention in rice paddies and removal of pollutant nitrogen in constructed wetlands therefore share a reac-

tion basis but differ in the appropriate configuration of oxygen and carbon supply [61]. Two further nitrogen pathways depend on the same spatial arrangement. Anaerobic ammonium oxidation has been detected in marsh, lake-shore, and paddy rhizosphere habitats where ammonium and nitrite meet within anoxic microsites [62,63], and nitrate reduction can terminate either in dinitrogen or in nitrous oxide, with carbon form and oxygen concentration jointly controlling the N_2O/N_2 ratio [64]. Therefore, nitrogen removal and greenhouse gas production are coupled outcomes of the same redox configuration.

Symbiotic and free-living nitrogen fixation add a further link between oxygen and the nitrogen cycle and correspond to the largest keyword cluster, which grouped nitrogen fixation, rhizobium, symbiosis, nodule, and oxygen [65]. Nitrogenase is inactivated by oxygen, yet nitrogen fixation is energetically expensive and depends on respiratory flux, creating a requirement to reconcile oxygen exclusion with oxygen supply [66]. In legume root nodules, this is achieved through spatial and biochemical separation: an oxygen diffusion barrier together with the oxygen-binding protein leghemoglobin buffers free oxygen to the nanomolar range while sustaining respiratory flux, and elimination of leghemoglobin raises the free oxygen concentration in nodules, lowers the ATP/ADP ratio, and abolishes nitrogen fixation [67–69]. Bacteroid respiration under these conditions proceeds through a high-affinity cbb3-type terminal oxidase with a Km for oxygen in the nanomolar range [70], and the nif and fix genes are governed by oxygen-responsive regulators that activate the fixation machinery only under microaerobic conditions [71,72]. Free-living nitrogen fixation is also constrained by oxygen sensitivity and energy demand, with oxygen, available carbon, and combined nitrogen regulating its activity [73]. Attempts to transfer nitrogen fixation to cereal-associated bacteria likewise identify oxygen protection of nitrogenase and the energy cost of fixation as central constraints [74]. These observations connect the symbiotic nitrogen fixation cluster to the same oxygen gradients that govern nitrification and denitrification, and they anticipate the iron-coupled nitrogen fixation considered next.

4.2.3. Iron and Manganese as Redox Hubs

Iron plaque extends these microsite connections to interactions between minerals and organic carbon. When oxygen released from roots encounters Fe(II) supplied from the surrounding soil, chemical and microbial oxidation can produce iron deposits on root surfaces. Early culture-kinetic studies under microaerobic conditions distinguished biological oxidation from abiotic reactions, showing that iron-oxidizing bacteria contribute to the formation of this interface while also competing for oxygen [75]. More recent cultivar comparisons combined root aeration traits, oxygen imaging, iron speciation, and ^{14}C tracing, linking stronger oxygen loss with greater iron-plaque accumulation and organic carbon retention [76]. Mechanistically, newly formed iron minerals in oxidized zones can bind organic carbon through sorption and coprecipitation, reducing the microbial availability of some substrates and linking plant oxygen supply to mineral-associated carbon formation [77].

The effects of iron plaque on carbon also depend on its properties as an electron acceptor and a medium for electron transfer. In rice experiments with pre-induced iron plaque, root-surface sterilization, ^{13}C-glucose tracing, and iron addition or chelation treatments supported the involvement of Fe(III) reduction in microbial respiration and enhanced oxidation of available organic carbon [78]. Further strain cocultures, methanogenesis inhibition, and mineral-addition experiments supported the interpretation that some conductive or semiconductive minerals in iron plaque facilitate interspecies electron transfer and syntrophic methanogenesis [79]. Plaque-associated carbon retention, carbon mineralization, and increased methane production thus correspond to processes involving mineral association, electron-acceptor use, and microbial cooperation, respectively. Their relative contributions

vary with mineral composition, substrate supply, and redox conditions. The expansion of research from plaque abundance and sorption to iron-speciation turnover and electron flow also makes it necessary to evaluate carbon stabilization alongside greenhouse gas budgets. Because Fe(III) reduction is energetically more favorable than sulfate reduction and methanogenesis, microbial Fe(III) oxide reduction can suppress both processes in vegetated wetland sediments so that iron turnover competes with the sulfate and methane pathways for the same electron donors [80].

Iron cycling provides a further connection to nitrogen fixation. In a hydroponic rice model, the presence of iron plaque was associated with higher nitrogenase activity and plant ^{15}N accumulation. Nitrogen fixation was lower after partial plaque disruption or under continuous light or darkness than under alternating light–dark conditions. Combined ^{15}N-DNA stable isotope probing and metagenomic analysis further identified taxa participating in nitrogen assimilation with the potential for nitrogen fixation and extracellular electron transfer [81]. These findings support a process-level connection between iron-plaque redox turnover and nitrogen fixation, and suggest a mechanism linking energy provision through Fe(III) reduction to the high energy demand of nitrogen fixation. Nitrogen, carbon, and iron research can thus be connected through electron donors, electron acceptors, and energy metabolism, extending beyond separate changes in the abundance of individual elements.

Redox-driven iron cycling also controls phosphorus availability. Fe(III) reduction releases phosphate previously bound to iron minerals, whereas re-oxidation and plaque formation retain it again so that phosphorus availability fluctuates with the same redox changes that govern carbon and nitrogen cycling [54]. Phosphorus availability in turn modulates nitrogen transformation, with P stoichiometry altering the abundance of nitrogen-cycle genes in P-limited paddy soils [82]. In eutrophic seagrass sediments, iron, sulfur, and phosphorus cycling were closely coupled across the annual cycle [83], and in wetland rhizosphere soils, microbial community composition and activity controlled the partitioning of phosphorus among its forms [84].

In the rhizosphere, Fe(II)- and Mn(II)-oxidizing bacteria promote the formation of mixed Fe/Mn plaques on root surfaces, which adsorb and co-precipitate metal(loid)s and thereby modulate their uptake [85]. Phosphate binding by iron plaque also couples oxygen release to phosphorus availability in the sediment [55]. Microbial redox cycling of manganese further controls its own bioavailability and that of associated nutrients, particularly in calcareous soils where chemical oxidation would otherwise immobilize Mn [86]. Iron and manganese therefore act as a coupled redox buffer that links oxygen supply to carbon, nutrient, and contaminant turnover along the cascade (Figure 7b).

4.2.4. Sulfate Reduction and Methanogenesis

Sulfur cycling illustrates another connection across redox interfaces. In the seagrass rhizosphere, planar oxygen optodes and sulfide imaging showed that localized oxygen loss from young roots coincided with reduced sulfide concentrations [87]. Fluorescence in situ hybridization and community analysis also identified enrichment of cable bacteria in the root-hair zones of oxygen-releasing roots [27]. These filamentous microorganisms can link sulfide oxidation in anoxic zones to oxygen reduction in oxic zones through long-distance electron transfer so that the reactions do not depend entirely on direct contact between oxygen and sulfide at the same location [88]. Subsequent surveys detected cable bacteria in the rhizospheres of multiple aquatic plants and rice paddies, extending this connection across a wider range of plant–sediment interfaces [89]. Local sulfide removal can help protect roots, while its spatial extent varies with root age, light, and sulfide supply, illustrating spatial complementarity between root oxygen release and microbial electron transfer.

Methane processes further reveal the competitive relationship between oxygen and carbon supply. Early oxygen microprofiles, atmosphere-switching experiments, and gas-flux measurements established the importance of plant-mediated oxygen transport to the flooded rhizosphere for methane oxidation [90–94]. Subsequent culture-kinetic and coculture experiments showed that methanotroph access to this oxygen also depends on competition with heterotrophic microorganisms. In the rice-paddy strain systems examined, lower oxygen and acetate supply favored the competitive position of methanotrophs, whereas greater organic substrate supply could increase heterotrophic oxygen consumption and suppress methane oxidation [95]. Root exudates therefore have a dual role: they supply carbon for anaerobic decomposition and methanogenesis while also affecting methanotroph access to oxygen [96,97]. Together with the role of aerenchyma in methane transport [5], these findings indicate that rhizosphere methane budgets should be understood through the combined processes of production, oxidation, and transport, with regulation focused on matching oxygen and substrate availability within reaction microsites [98].

4.2.5. Contaminant Fate and Environmental Applications

Root-associated processes affect both organic-contaminant degradation, as shown for sulfonamides in constructed wetlands [99], and contaminant-element speciation, as shown for arsenic in the rice rhizosphere [100]. Rice microfluidic experiments in which cadmium sulfide was the main cadmium-bearing phase showed that oxidation associated with daytime oxygen loss promoted cadmium dissolution, while higher pH counteracted dissolution. Under anoxic conditions, microbial sulfide production could promote cadmium immobilization [101]. These findings connect heavy-metal research with sulfur transformations, oxygen fluctuations, and acid–base conditions, indicating that contaminant regulation requires attention to both solid-phase transformations and transport in the dissolved phase [102]. Sorption by iron plaque, sulfide precipitation, and oxidative dissolution represent different reaction steps [103,104]. Identifying the dominant step in a particular system is therefore necessary to explain why similar changes in oxygen supply may produce different contaminant responses [105]. Beyond arsenic and cadmium, iron plaque also retains Cu, Zn, Pb, and other metals so that plaque formation couples oxygen release to multi-metal sequestration in wetland and mine-waste settings [106]. Water management extends this control to mercury, where aerobic rice cultivation lowered mercury bioavailability and methylmercury accumulation by altering sulfate-reducing communities [107]. Inoculation with Fe-oxidizing and Mn-oxidizing bacteria enhanced plaque formation and reduced Cd and As accumulation in rice [108].

Redox conditions within the rhizosphere also govern the fate of organic contaminants, although this dimension is less frequently quantified than for inorganic pollutants. Aerobic and anaerobic zones support complementary degradation pathways, and their coexistence within millimeters of a root allows sequential or simultaneous aerobic and anaerobic steps in the same soil volume [109]. Plant-based remediation has long been proposed for soils and groundwater contaminated with organic materials [110], but its efficiency depends strongly on hydrology, sediment type, and plant species; therefore, the reported removal differs widely among wetland systems [111]. In sediments, combining macrophyte roots with a sediment microbial fuel cell increased degradation of high-molecular-weight polycyclic aromatic hydrocarbons relative to either component alone [112], consistent with coupling between root oxygen release, electron transfer, and contaminant oxidation.

The same redox interface operates in tidal and coastal wetlands, where water-level fluctuations impose frequent redox oscillations. In salt-marsh sediments, roots and burrowing macrofauna together structure sulfur and iron cycling [113], and mangrove wetlands emit methane and nitrous oxide at rates that vary strongly with substrate availability [114]. In

seagrass tissues, low-oxygen supply allows sulfide intrusion so that the oxygen status of the plant determines its exposure to a phytotoxin [115]. These interfaces are also used in engineered systems: plant microbial fuel cells exploit root-derived organic matter and oxygen release to generate current [116], and a biocathode placed in the rice rhizosphere can transfer electrons to root-released oxygen, which serves as the terminal electron acceptor [117].

4.3. Research Frontiers and Future Directions

The recent bursts of microbial community and reactive oxygen species, together with work on root exudates and iron plaque, direct attention to how plants and microorganisms jointly regulate their chemical environment. Resolving these interactions requires both spatially explicit observations and identification of the organisms and pathways responsible for transformations. Integration of sensing, imaging, and computational methods offers a route to connect these forms of evidence across scales [118]. Evidence availability nevertheless differs among habitat groups and scales, with plot- and field-scale validation lagging behind microsite observations, particularly for coastal, nodular, and aerobic systems (Figure 8).

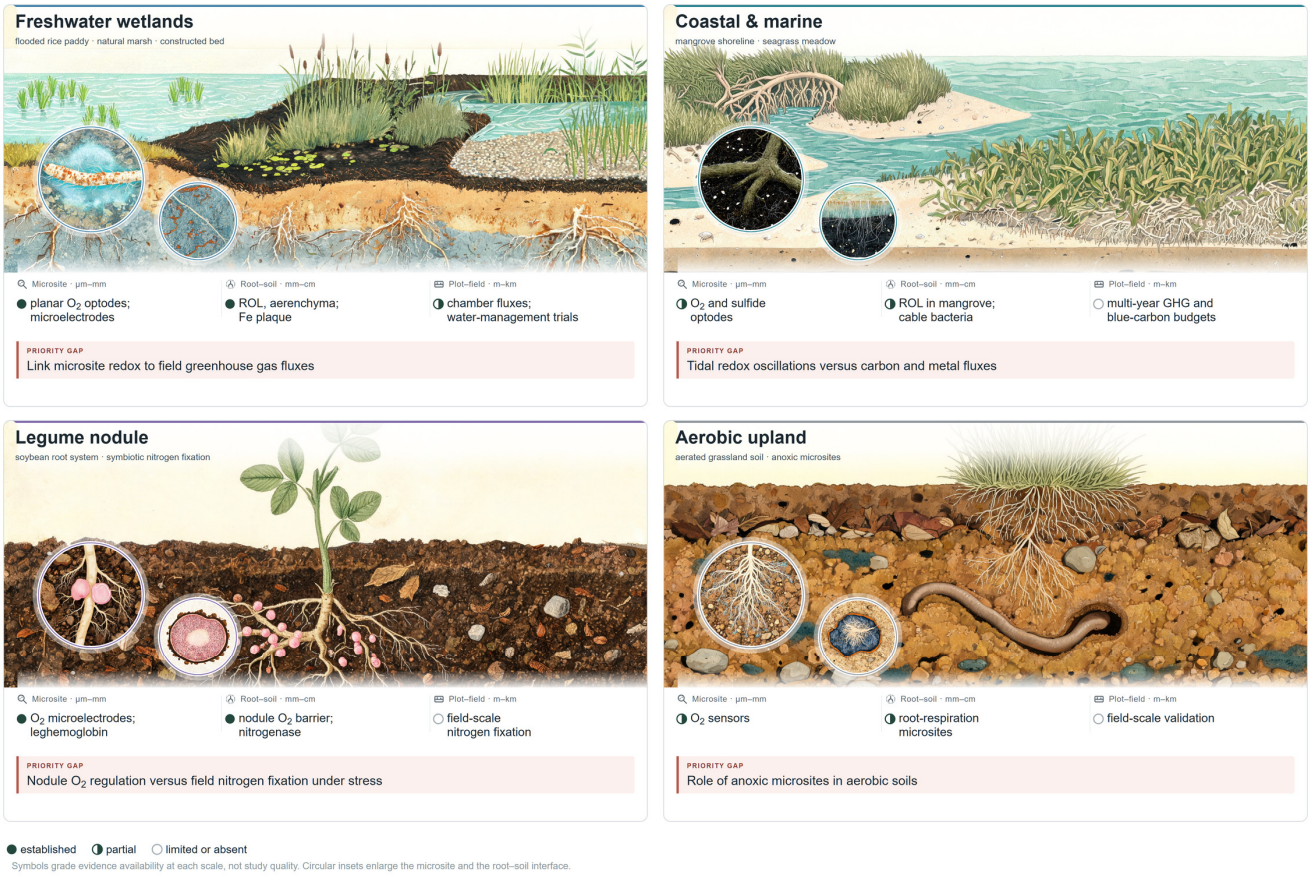


Figure 8. Evidence availability across spatial scales in rhizosphere oxygen research. Four habitat groups (freshwater wetlands, coastal and marine, legume nodule, and aerobic upland) are each shown at three nested scales (microsite, µm–mm; root–soil, mm–cm; plot–field, m–km), with one priority knowledge gap for each group. Symbols grade the availability of evidence at each scale—established (●), partial (◐), and limited or absent (○)—and do not grade study quality; circular insets enlarge the microsite and the root–soil interface. The figure was generated with the assistance of AI tools (TraeWork v0.1.69 Design mode for the figure design and layout, DeepSeek-V4.1-Flash for drafting, and Seedream 5.0 for image generation). The authors have verified the figure's content and take full responsibility for it.

Spatial observations are expanding from individual profiles to multivariable imaging and dynamic tracking [119]. Oxygen microelectrodes can relate concentration gradients between the root surface and bulk soil to process activity [6,90,120,121]. Planar optical sensing extends observations to two-dimensional areas; early imaging of plant tissues and roots demonstrated the ability to identify localized oxygen consumption and production [122]. Planar optodes and two-dimensional chemical imaging can further resolve gradients of multiple solutes simultaneously [123–125]. Subsequent integration of oxygen imaging with sulfide distributions, fluorescence in situ hybridization, and ^{14}C tracing has linked oxygen microsites to microbial colonization and carbon fate [27,76]. Microfluidic devices further bring growing roots, light–dark transitions, and chemical conditions into controlled systems, capturing temporal changes in processes such as root-tip movement and cadmium dissolution [29,101,126]. Together, these methods allow researchers to determine where reactions occur, how long they persist, and which biological or chemical changes accompany them.

Functional identification requires connecting community information with material transformations. Amplicon sequencing and metagenomics provide information on taxonomic composition and functional potential, respectively. The amplicon-denoising method DADA2 improves the resolution of sequence variants [127]. QIIME 2 workflows integrate quality control, denoising, taxonomic assignment, and diversity analysis [128]. Stable isotope probing links labeled-substrate use to particular microorganisms, providing a basis for connecting community identity with material transformations [129]. Combining ^{13}C-substrate tracing with root-surface sterilization, iron addition, or chelation can test the microbial origin and iron dependence of plaque-associated respiration [78]. Combining ^{15}N-DNA stable isotope probing with metagenomic binning links nitrogen-assimilating taxa to their metabolic potential [81]. Because labels can reach organisms other than the initial substrate users through cross-feeding, omics and tracing results can be complemented by strain cocultures, functional inhibition, and process-rate measurements to distinguish direct effects from community cooperation. Such combinations also provide experimental routes to test associations suggested by co-occurrence networks.

Research on biochar illustrates a shift in material-based regulation from comparing treatment effects to explaining reaction mechanisms. A two-season rice-field experiment showed that biochar and a nitrification inhibitor affected nitrogen-loss pathways differently: biochar increased denitrification losses as N_2 and ammonia volatilization, whereas the nitrification inhibitor reduced denitrification losses [130]. More recent iron plaque–biochar experiments connected measurements of N_2O and N_2 with functional gene expression and material electrochemical properties. As biochar became more oxidized and its electron-donating capacity declined, its suppression of plaque-associated N_2O accumulation weakened, supporting a role for electron transfer in N_2O reduction [131]. Material selection should therefore be linked to specific reaction pathways and product partitioning, with distinctions among the goals of greenhouse gas mitigation, total nitrogen retention, and crop growth. Existing synthesis also indicates that biochar effects on N_2O are jointly constrained by soil texture, substrate availability, pH, aeration, and microbial activity [132].

Future research can strengthen the connection between microsite mechanisms and ecosystem functioning. At the process level, simultaneous observations of oxygen distributions, root exudates, iron speciation, and microbial activity could identify reaction shifts as redox interfaces move. At the biological level, combined inoculation and oxygen-supply manipulations could resolve bidirectional regulation between root traits and microbial functions. At the application level, mechanisms identified in microfluidic devices or rhizoboxes should be tested over complete growing seasons and under fluctuating water conditions, with joint evaluation of carbon retention, CH_4 and N_2O fluxes, nitrogen use, and contaminant bioavailability.

4.4. Limitations

Bibliometric indicators describe publication activity and relationships among records; they do not measure experimental quality or establish causal links between research themes. Citation counts accumulate with time, and average publication years depend on the temporal composition of each country's or topic's publications. Author-name variants and historical differences in keyword availability also affect the resolution of collaboration and temporal analyses. In particular, recent burst intervals remain bounded by the 2025 endpoint and cannot establish whether attention will persist. The mechanistic literature spans flooded soils, wetlands, aerated rhizospheres, and legume nodules, where oxygen supply, substrates, and biological organization differ. Process relationships identified in one setting therefore require context-specific interpretation before they are extended to another.

5. Conclusions

Research on rhizosphere oxygen environments and microorganisms has expanded from a substantial foundation in oxygen-sensitive nitrogen fixation to a broader set of questions involving wetland aeration, microbial communities, iron transformations, and plant chemical regulation. The recent rise in publication output is accompanied by collaborations linking physiological investigations with soil and environmental applications. Across the six keyword themes, oxygen supply and biological oxygen consumption provide a recurring basis for understanding where microbial transformations occur, while substrate availability and redox dynamics determine their outcomes. Iron-plaque studies illustrate why the same root-associated mineral interface can support carbon retention, carbon oxidation, or methane production under different conditions. Future work should connect spatially resolved oxygen measurements with microbial functional tests and isotope tracing, and relate these mechanisms to field-scale nutrient retention, contaminant behavior, and greenhouse gas fluxes.

Supplementary Materials: The following supporting information can be downloaded at: https://www.mdpi.com/article/10.3390/environments13110605/s1, Supplementary Methods S1–S9 describe the search, screening, normalization, analysis, data availability, and screening-model specifications. Figure S1 reports the record-selection flow; Figure S2 shows annual-count model diagnostics. Tables S1–S25 provide thesauri, network parameters, bibliometric rankings, annual counts, keyword bursts and coverage, scope checks, model comparisons, and representative mechanistic studies. The record-level screening ledger, the derived tables, and the analysis scripts are available from the corresponding author upon reasonable request.

Author Contributions: D.Y.: Conceptualization, Investigation, Visualization, Formal Analysis, Writing—Original Draft; Y.L.: Conceptualization, Investigation, Writing—Review and Editing; Y.C.: Writing—Review and Editing; L.F.: Writing—Review and Editing; Y.Z.: Validation; J.L.: Writing—Review and Editing; H.L.: Resources, Funding Acquisition, Writing—Review and Editing; H.H.: Conceptualization, Supervision, Writing—Review and Editing. All authors have read and agreed to the published version of the manuscript.

Funding: This work was funded by the National Key R&D Program of China (2022YFF0803100); the National Natural Science Foundation of China (U25A20801); and XMU Undergraduate Innovation Training Programs (2026X898).

Data Availability Statement: The bibliographic records were obtained from the Web of Science Core Collection under a Clarivate license that does not permit redistribution of raw or record-level metadata; the complete bibliographic dataset and the record-level screening ledger therefore cannot be shared publicly. Data supporting the conclusions of this article are provided in the Supplementary Materials (Tables S1–S25; Figures S1 and S2), together with the search strings and retrieval dates documented in Supplementary Methods S1, so that the collection can be reconstructed by users with licensed access; the accession-number list is available from the corresponding author upon reasonable

request. The analysis scripts are available from the corresponding author upon reasonable request. Access to the record-level ledger is subject to the applicable Web of Science license conditions.

Acknowledgments: We would like to express our gratitude to Jun Liu from Xiamen University for her help during the implementation of this research. During the preparation of this manuscript, the authors used Intern-Decision-4B and DeepSeek-V4.1-Flash for scope-screening (Section 2.2), TraeWork v0.1.69 Design mode for the design and layout of Figures 6–8, Seedream 5.0 for image generation of the schematic syntheses in Figures 6–8, and DeepSeek-V4.1-Flash for drafting and language editing. The authors reviewed and edited all AI-assisted output and take full responsibility for the content of this publication.

Conflicts of Interest: The authors declare no conflicts of interest.

References

1. Philippot, L.; Raaijmakers, J.M.; Lemanceau, P.; van der Putten, W.H. Going back to the roots: The microbial ecology of the rhizosphere. *Nat. Rev. Microbiol.* **2013**, *11*, 789–799. [CrossRef] [PubMed]
2. Bais, H.P.; Weir, T.L.; Perry, L.G.; Gilroy, S.; Vivanco, J.M. The role of root exudates in rhizosphere interactions with plants and other organisms. *Annu. Rev. Plant Biol.* **2006**, *57*, 233–266. [CrossRef] [PubMed]
3. Compant, S.; Cassan, F.; Kostić, T.; Johnson, L.; Brader, G.; Trognitz, F.; Sessitsch, A. Harnessing the plant microbiome for sustainable crop production. *Nat. Rev. Microbiol.* **2025**, *23*, 9–23. [CrossRef] [PubMed]
4. Bulgarelli, D.; Schlaeppi, K.; Spaepen, S.; van Themaat, E.V.L.; Schulze-Lefert, P. Structure and functions of the bacterial microbiota of plants. *Annu. Rev. Plant Biol.* **2013**, *64*, 807–838. [CrossRef] [PubMed]
5. Colmer, T.D. Long-distance transport of gases in plants: A perspective on internal aeration and radial oxygen loss from roots. *Plant Cell Environ.* **2003**, *26*, 17–36. [CrossRef]
6. Li, Y.; Wang, X. Root-induced changes in radial oxygen loss, rhizosphere oxygen profile, and nitrification of two rice cultivars in Chinese red soil regions. *Plant Soil* **2013**, *365*, 115–126. [CrossRef]
7. Kögel-Knabner, I.; Amelung, W.; Cao, Z.; Fiedler, S.; Frenzel, P.; Jahn, R.; Kalbitz, K.; Kölbl, A.; Schloter, M. Biogeochemistry of paddy soils. *Geoderma* **2010**, *157*, 1–14. [CrossRef]
8. Fan, Y.; Sun, S.; He, S. Iron plaque formation and its effect on key elements cycling in constructed wetlands: Functions and outlooks. *Water Res.* **2023**, *235*, 119837. [CrossRef] [PubMed]
9. Donthu, N.; Kumar, S.; Mukherjee, D.; Pandey, N.; Lim, W.M. How to conduct a bibliometric analysis: An overview and guidelines. *J. Bus. Res.* **2021**, *133*, 285–296. [CrossRef]
10. Sun, S.; Xue, R.; Liu, M.; Wang, L.; Zhang, W. Research progress and hotspot analysis of rhizosphere microorganisms based on bibliometrics from 2012 to 2021. *Front. Microbiol.* **2023**, *14*, 1085387. [CrossRef] [PubMed]
11. Wang, Y.; Bai, J.; Zhang, L.; Liu, H.; Wang, W.; Liu, Z.; Zhang, G. Advances in studies on the plant rhizosphere microorganisms in wetlands: A visualization analysis based on CiteSpace. *Chemosphere* **2023**, *317*, 137860. [CrossRef] [PubMed]
12. Page, M.J.; McKenzie, J.E.; Bossuyt, P.M.; Boutron, I.; Hoffmann, T.C.; Mulrow, C.D.; Shamseer, L.; Tetzlaff, J.M.; Akl, E.A.; Brennan, S.E.; et al. The PRISMA 2020 statement: An updated guideline for reporting systematic reviews. *BMJ* **2021**, *372*, n71. [CrossRef] [PubMed]
13. van Eck, N.J.; Waltman, L. Software survey: VOSviewer, a computer program for bibliometric mapping. *Scientometrics* **2010**, *84*, 523–538. [CrossRef] [PubMed]
14. Waltman, L.; van Eck, N.J.; Noyons, E.C.M. A unified approach to mapping and clustering of bibliometric networks. *J. Informetr.* **2010**, *4*, 629–635. [CrossRef]
15. Kleinberg, J. Bursty and hierarchical structure in streams. *Data Min. Knowl. Discov.* **2003**, *7*, 373–397. [CrossRef]
16. Saitou, N.; Nei, M. The neighbor-joining method: A new method for reconstructing phylogenetic trees. *Mol. Biol. Evol.* **1987**, *4*, 406–425. [CrossRef] [PubMed]
17. Felsenstein, J. Confidence limits on phylogenies: An approach using the bootstrap. *Evolution* **1985**, *39*, 783–791. [CrossRef] [PubMed]
18. Caporaso, J.G.; Kuczynski, J.; Stombaugh, J.; Bittinger, K.; Bushman, F.D.; Costello, E.K.; Fierer, N.; Peña, A.G.; Goodrich, J.K.; Gordon, J.I.; et al. QIIME allows analysis of high-throughput community sequencing data. *Nat. Methods* **2010**, *7*, 335–336. [CrossRef] [PubMed]
19. Edwards, J.; Johnson, C.; Santos-Medellín, C.; Lurie, E.; Podishetty, N.K.; Bhatnagar, S.; Eisen, J.A.; Sundaresan, V. Structure, variation, and assembly of the root-associated microbiomes of rice. *Proc. Natl. Acad. Sci. USA* **2015**, *112*, E911–E920. [CrossRef] [PubMed]

20. Zhalnina, K.; Louie, K.B.; Hao, Z.; Mansoori, N.; da Rocha, U.N.; Shi, S.; Cho, H.; Karaoz, U.; Loqué, D.; Bowen, B.P.; et al. Dynamic root exudate chemistry and microbial substrate preferences drive patterns in rhizosphere microbial community assembly. *Nat. Microbiol.* **2018**, *3*, 470–480. [CrossRef] [PubMed]
21. Kuzyakov, Y.; Blagodatskaya, E. Microbial hotspots and hot moments in soil: Concept & review. *Soil Biol. Biochem.* **2015**, *83*, 184–199. [CrossRef]
22. Srivastava, A.K.; Singh, R.D.; Pandey, G.K.; Mukherjee, P.K.; Foyer, C.H. Unravelling the Molecular Dialogue of Beneficial Microbe-Plant Interactions. *Plant Cell Environ.* **2025**, *48*, 2534–2548. [CrossRef] [PubMed]
23. Jiang, O.Y.; Li, L.; Duan, G.L.; Gustave, W.; Zhai, W.W.; Zou, L.N.; An, X.; Tang, X.J.; Xu, J.M. Root exudates increased arsenic mobility and altered microbial community in paddy soils. *J. Environ. Sci.* **2023**, *127*, 410–420. [CrossRef] [PubMed]
24. Hu, L.Y.; Yang, Y.; Wu, H.; Tang, M.J.; Xie, X.G.; Dai, C.C. *Phomopsis liquidambaris* Increases Rice Mineral Uptake Under Waterlogging Condition via the Formation of Well-Developed Root Aerenchyma. *J. Plant Growth Regul.* **2022**, *41*, 1758–1772. [CrossRef]
25. Hu, L.-Y.; Li, D.; Sun, K.; Cao, W.; Fu, W.-Q.; Zhang, W.; Dai, C.-C. Mutualistic fungus *Phomopsis liquidambari* increases root aerenchyma formation through auxin-mediated ethylene accumulation in rice (*Oryza sativa* L.). *Plant Physiol. Biochem.* **2018**, *130*, 367–376. [CrossRef] [PubMed]
26. Zhang, Q.H.; Huang, J.N.; Dzakpasu, M.; Gao, Z.; Zhou, W.D.; Zhu, R.T.; Xiong, J.Q. Assessment of plants radial oxygen loss for nutrients and organic matter removal in full-scale constructed wetlands treating municipal effluents. *Bioresour. Technol.* **2022**, *360*, 127545. [CrossRef] [PubMed]
27. Martin, B.C.; Bougoure, J.; Ryan, M.H.; Bennett, W.W.; Colmer, T.D.; Joyce, N.K.; Olsen, Y.S.; Kendrick, G.A. Oxygen loss from seagrass roots coincides with colonisation of sulphide-oxidising cable bacteria and reduces sulphide stress. *ISME J.* **2019**, *13*, 707–719. [CrossRef] [PubMed]
28. Kirk, G.J.D.; Kronzucker, H.J. The potential for nitrification and nitrate uptake in the rhizosphere of wetland plants: A modelling study. *Ann. Bot.* **2005**, *96*, 639–646. [CrossRef] [PubMed]
29. Lacroix, E.M.; Ceriotti, G.; Garrido-Sanz, D.; Borisov, S.M.; Berg, J.S.; Keel, C.; de Anna, P.; Keiluweit, M. Root and microbial contributions to anoxic microsite formation in the rhizosphere: A microfluidic approach. *New Phytol.* **2026**, *250*, 3486–3498. [CrossRef] [PubMed]
30. Colmer, T.D.; Voesenek, L.A.C.J. Flooding tolerance: Suites of plant traits in variable environments. *Funct. Plant Biol.* **2009**, *36*, 665–681. [CrossRef] [PubMed]
31. Martínez-Arias, C.; Witzell, J.; Solla, A.; Martin, J.A.; Rodríguez-Calcerrada, J. Beneficial and pathogenic plant–microbe interactions during flooding stress. *Plant Cell Environ.* **2022**, *45*, 2875–2897. [CrossRef] [PubMed]
32. Edwards, J.; Santos-Medellín, C.; Nguyen, B.; Kilmer, J.; Liechty, Z.; Veliz, E.; Ni, J.; Phillips, G.; Sundaresan, V. Soil domestication by rice cultivation results in plant-soil feedback through shifts in soil microbiota. *Genome Biol.* **2019**, *20*, 221. [CrossRef] [PubMed]
33. Kumar, A.; Singh, S.; Gaurav, A.K.; Srivastava, S.; Verma, J.P. Plant growth-promoting bacteria: Biological tools for the mitigation of salinity stress in plants. *Front. Microbiol.* **2020**, *11*, 1216. [CrossRef] [PubMed]
34. Santos, R.; Hérouart, D.; Sigaud, S.; Touati, D.; Puppo, A. Oxidative burst in alfalfa-*Sinorhizobium meliloti* symbiotic interaction. *Mol. Plant-Microbe Interact.* **2001**, *14*, 86–89. [CrossRef] [PubMed]
35. Pauly, N.; Pucciariello, C.; Mandon, K.; Innocenti, G.; Jamet, A.; Baudouin, E.; Hérouart, D.; Frendo, P.; Puppo, A. Reactive oxygen and nitrogen species and glutathione: Key players in the legume-*Rhizobium symbiosis*. *J. Exp. Bot.* **2006**, *57*, 1769–1776. [CrossRef] [PubMed]
36. Nostadt, R.; Hilbert, M.; Nizam, S.; Rovenich, H.; Wawra, S.; Martin, J.; Küpper, H.; Mijovilovich, A.; Ursinus, A.; Langen, G.; et al. A secreted fungal histidine- and alanine-rich protein regulates metal ion homeostasis and oxidative stress. *New Phytol.* **2020**, *227*, 1174–1188. [CrossRef] [PubMed]
37. White, J.F.; Kingsley, K.L.; Verma, S.K.; Kowalski, K.P. Rhizophagy Cycle: An Oxidative Process in Plants for Nutrient Extraction from Symbiotic Microbes. *Microorganisms* **2018**, *6*, 95. [CrossRef] [PubMed]
38. Ruiz-Lozano, J.M.; Collados, C.; Barea, J.M.; Azcón, R. Arbuscular mycorrhizal symbiosis can alleviate drought-induced nodule senescence in soybean plants. *New Phytol.* **2001**, *151*, 493–502. [CrossRef]
39. Schützendübel, A.; Polle, A. Plant responses to abiotic stresses: Heavy metal-induced oxidative stress and protection by mycorrhization. *J. Exp. Bot.* **2002**, *53*, 1351–1365. [CrossRef]
40. Hinsinger, P.; Bengough, A.G.; Vetterlein, D.; Young, I.M. Rhizosphere: Biophysics, biogeochemistry and ecological relevance. *Plant Soil* **2009**, *321*, 117–152. [CrossRef]
41. Jorgensen, C.J.; Struwe, S.; Elberling, B. Temporal trends in N_2O flux dynamics in a Danish wetland—Effects of plant-mediated gas transport of N_2O and O_2 following changes in water level and soil mineral-N availability. *Glob. Change Biol.* **2012**, *18*, 210–222. [CrossRef]
42. Koop-Jakobsen, K.; Wenzhöfer, F. The Dynamics of Plant-Mediated Sediment Oxygenation in *Spartina anglica* Rhizospheres-a Planar Optode Study. *Estuaries Coasts* **2015**, *38*, 951–963. [CrossRef]

43. Schmidt, H.; Eickhorst, T.; Tippkötter, R. Monitoring of root growth and redox conditions in paddy soil rhizotrons by redox electrodes and image analysis. *Plant Soil* **2011**, *341*, 221–232. [CrossRef]
44. Münch, C.; Kuschk, P.; Röske, I. Root stimulated nitrogen removal: Only a local effect or important for water treatment? *Water Sci. Technol.* **2005**, *51*, 185–192. [CrossRef]
45. Gibberd, M.R.; Gray, J.D.; Cocks, P.S.; Colmer, T.D. Waterlogging tolerance among a diverse range of Trifolium accessions is related to root porosity, lateral root formation and 'aerotropic rooting'. *Ann. Bot.* **2001**, *88*, 579–589. [CrossRef]
46. Colmer, T.D.; Kotula, L.; Malik, A.; Takahashi, H.; Konnerup, D.; Nakazono, M.; Pedersen, O. Rice acclimation to soil flooding: Low concentrations of organic acids can trigger a barrier to radial oxygen loss in roots. *Plant Cell Environ.* **2019**, *42*, 2183–2197. [CrossRef] [PubMed]
47. Hoefer, C.; Santner, J.; Puschenreiter, M.; Wenzel, W.W. Localized Metal Solubilization in the Rhizosphere of *Salix smithiana* upon Sulfur Application. *Environ. Sci. Technol.* **2015**, *49*, 4522–4529. [CrossRef] [PubMed]
48. Zhu, K.; Bruun, S.; Larsen, M.; Glud, R.N.; Jensen, L.S. Heterogeneity of O_2 dynamics in soil amended with animal manure and implications for greenhouse gas emissions. *Soil Biol. Biochem.* **2015**, *84*, 96–106. [CrossRef]
49. Wiessner, A.; Kappelmeyer, U.; Kuschk, P.; Kästner, M. Influence of the redox condition dynamics on the removal efficiency of a laboratory-scale constructed wetland. *Water Res.* **2005**, *39*, 248–256. [CrossRef] [PubMed]
50. Guo, D.; Zhang, J.Y.; Bian, W.; Chi, Y.B.; Li, B.; Ren, Q.T.; Yang, L.; Lan, J.; Ren, Y.X. Quantifying the underestimated plant potential for phosphorus removal in constructed wetlands: Revealing the mediating mechanism of radial oxygen loss. *Water Res.* **2025**, *284*, 123923. [CrossRef] [PubMed]
51. Jones, D.L. Organic acids in the rhizosphere—A critical review. *Plant Soil* **1998**, *205*, 25–44. [CrossRef]
52. Husson, O. Redox potential (Eh) and pH as drivers of soil/plant/microorganism systems: A transdisciplinary overview pointing to integrative opportunities for agronomy. *Plant Soil* **2013**, *362*, 389–417. [CrossRef]
53. Keiluweit, M.; Wanzek, T.; Kleber, M.; Nico, P.; Fendorf, S. Anaerobic microsites have an unaccounted role in soil carbon stabilization. *Nat. Commun.* **2017**, *8*, 1771. [CrossRef] [PubMed]
54. Wu, S.B.; Vymazal, J.; Brix, H. Critical Review: Biogeochemical Networking of Iron in Constructed Wetlands for Wastewater Treatment. *Environ. Sci. Technol.* **2019**, *53*, 7930–7944. [CrossRef] [PubMed]
55. Christensen, K.K.; Wigand, C. Formation of root plaques and their influence on tissue phosphorus content in *Lobelia dortmanna*. *Aquat. Bot.* **1998**, *61*, 111–122. [CrossRef]
56. Bodelier, P.; Libochant, J.A.; Blom, C.; Laanbroek, H.J. Dynamics of nitrification and denitrification in root-oxygenated sediments and adaptation of ammonia-oxidizing bacteria to low-oxygen or anoxic habitats. *Appl. Environ. Microbiol.* **1996**, *62*, 4100–4107. [CrossRef] [PubMed]
57. Bai, S.; Chen, J.; Guo, M.; Ren, N.; Zhao, X. Vertical-scale spatial influence of radial oxygen loss on rhizosphere microbial community in constructed wetland. *Environ. Int.* **2023**, *171*, 107690. [CrossRef] [PubMed]
58. Stottmeister, U.; Wiessner, A.; Kuschk, P.; Kappelmeyer, U.; Kästner, M.; Bederski, O.; Müller, R.A.; Moormann, H. Effects of plants and microorganisms in constructed wetlands for wastewater treatment. *Biotechnol. Adv.* **2003**, *22*, 93–117. [CrossRef] [PubMed]
59. Brix, H. Do macrophytes play a role in constructed treatment wetlands? *Water Sci. Technol.* **1997**, *35*, 11–17. [CrossRef]
60. Hu, X.J.; Xie, J.X.; Xie, H.J.; Huo, J.Y.; Wu, H.M.; Hu, Z.; Xue, K.; Song, M.Y.; Liang, S.; Zhang, J. Towards a better and more complete understanding of microbial nitrogen transformation processes in the rhizosphere of subsurface flow constructed wetlands: Effect of plant root activities. *Chem. Eng. J.* **2023**, *463*, 142455. [CrossRef]
61. Tanner, C.C.; Kadlec, R.H.; Gibbs, M.M.; Sukias, J.P.S.; Nguyen, M.L. Nitrogen processing gradients in subsurface-flow treatment wetlands—Influence of wastewater characteristics. *Ecol. Eng.* **2002**, *18*, 499–520. [CrossRef]
62. Humbert, S.; Tarnawski, S.; Fromin, N.; Mallet, M.P.; Aragno, M.; Zopfi, J. Molecular detection of anammox bacteria in terrestrial ecosystems: Distribution and diversity. *ISME J.* **2010**, *4*, 450–454. [CrossRef] [PubMed]
63. Nie, S.A.; Li, H.; Yang, X.R.; Zhang, Z.J.; Weng, B.S.; Huang, F.Y.; Zhu, G.B.; Zhu, Y.G. Nitrogen loss by anaerobic oxidation of ammonium in rice rhizosphere. *ISME J.* **2015**, *9*, 2059–2067. [CrossRef] [PubMed]
64. Morley, N.; Baggs, E.M. Carbon and oxygen controls on N_2O and N_2 production during nitrate reduction. *Soil Biol. Biochem.* **2010**, *42*, 1864–1871. [CrossRef]
65. Jones, K.M.; Kobayashi, H.; Davies, B.W.; Taga, M.E.; Walker, G.C. How rhizobial symbionts invade plants: The Sinorhizobium-Medicago model. *Nat. Rev. Microbiol.* **2007**, *5*, 619–633. [CrossRef] [PubMed]
66. Meilhoc, E.; Boscari, A.; Pauly, N.; Lepetit, M.; Frendo, P.; Bruand, C.; Puppo, A.; Brouquisse, R. Oxygen and derived reactive species in legume-rhizobia interactions: Paradoxes and dual roles. *J. Exp. Bot.* **2025**, *76*, 3758–3773. [CrossRef] [PubMed]
67. Ott, T.; van Dongen, J.T.; Günther, C.; Krusell, L.; Desbrosses, G.; Vigeolas, H.; Bock, V.; Czechowski, T.; Geigenberger, P.; Udvardi, M.K. Symbiotic leghemoglobins are crucial for nitrogen fixation in legume root nodules but not for general plant growth and development. *Curr. Biol.* **2005**, *15*, 531–535. [CrossRef] [PubMed]
68. Larrainzar, E.; Villar, I.; Rubio, M.C.; Pérez-Rontomé, C.; Huertas, R.; Sato, S.; Mun, J.H.; Becana, M. Hemoglobins in the legume-*Rhizobium symbiosis*. *New Phytol.* **2020**, *228*, 472–484. [CrossRef] [PubMed]

69. James, E.K.; Sprent, J.I.; Minchin, F.R.; Brewin, N.J. Intercellular location of glycoprotein in soybean nodules—Effect of altered rhizosphere oxygen concentration. *Plant Cell Environ.* **1991**, *14*, 467–476. [CrossRef]
70. Preisig, O.; Zufferey, R.; Thöny-Meyer, L.; Appleby, C.A.; Hennecke, H. A high-affinity cbb3-type cytochrome oxidase terminates the symbiosis-specific respiratory chain of *Bradyrhizobium japonicum*. *J. Bacteriol.* **1996**, *178*, 1532–1538. [CrossRef] [PubMed]
71. Fischer, H.M. Genetic regulation of nitrogen fixation in rhizobia. *Microbiol. Rev.* **1994**, *58*, 352–386. [CrossRef] [PubMed]
72. Pessi, G.; Ahrens, C.H.; Rehrauer, H.; Lindemann, A.; Hauser, F.; Fischer, H.M.; Hennecke, H. Genome-wide transcript analysis of *Bradyrhizobium japonicum* bacteroids in soybean root nodules. *Mol. Plant-Microbe Interact.* **2007**, *20*, 1353–1363. [CrossRef] [PubMed]
73. Reed, S.C.; Cleveland, C.C.; Townsend, A.R. Functional ecology of free-living nitrogen fixation: A contemporary perspective. *Annu. Rev. Ecol. Evol. Syst.* **2011**, *42*, 489–512. [CrossRef]
74. Ryu, M.-H.; Zhang, J.; Toth, T.; Khokhani, D.; Geddes, B.A.; Mus, F.; Garcia-Costas, A.; Peters, J.W.; Poole, P.S.; Ané, J.-M.; et al. Control of nitrogen fixation in bacteria that associate with cereals. *Nat. Microbiol.* **2020**, *5*, 314–330. [CrossRef] [PubMed]
75. Neubauer, S.C.; Emerson, D.; Megonigal, J.P. Life at the energetic edge: Kinetics of circumneutral iron oxidation by lithotrophic iron-oxidizing bacteria isolated from the wetland-plant rhizosphere. *Appl. Environ. Microbiol.* **2002**, *68*, 3988–3995. [CrossRef] [PubMed]
76. Wei, L.; Rong, X.; Yuan, H.; Li, Y.; Fan, X.; Ling, N.; Zhu, Z.; Razavi, B.S.; Kuzyakov, Y.; Kim, P.J.; et al. Carbon stabilization by iron plaque on rice roots: The role of oxygen loss. *Soil Biol. Biochem.* **2025**, *210*, 109947. [CrossRef]
77. Wei, L.; Zhu, Z.K.; Razavi, B.S.; Xiao, M.L.; Dorodnikov, M.; Fan, L.C.; Yuan, H.Z.; Yurtaev, A.; Luo, Y.; Cheng, W.G.; et al. Visualization and quantification of carbon "rusty sink" by rice root iron plaque: Mechanisms, functions, and global implications. *Glob. Change Biol.* **2022**, *28*, 6711–6727. [CrossRef] [PubMed]
78. Yao, J.; Qin, S.; Liu, T.; Clough, T.J.; Wrage-Mönnig, N.; Luo, J.; Hu, C.; Ge, T.; Zhou, S. Rice root Fe plaque enhances oxidation of microbially available organic carbon via Fe(III) reduction-coupled microbial respiration. *Soil Biol. Biochem.* **2022**, *167*, 108568. [CrossRef]
79. Yao, J.; Xie, M.; Yu, L.; Liu, T.; Clough, T.J.; Wrage-Mönnig, N.; Luo, J.; Hu, C.; Ge, T.; Zhou, S.; et al. Rice root Fe plaque increases paddy soil CH_4 emissions via the promotion of electron transfer for syntrophic methanogenesis. *Soil Biol. Biochem.* **2024**, *191*, 109332. [CrossRef]
80. Roden, E.E.; Wetzel, R.G. Organic carbon oxidation and suppression of methane production by microbial Fe(III) oxide reduction in vegetated and unvegetated freshwater wetland sediments. *Limnol. Oceanogr.* **1996**, *41*, 1733–1748. [CrossRef]
81. Jia, R.; Yu, L.; Wang, M.; Wu, Y.; Liu, S.; Zhong, S.; Zhou, S. Unveiling the crucial role of rice root iron plaque in enhancing biological nitrogen fixation via ^{15}N-labeling DNA-SIP and metagenomics in a model study. *Biol. Fertil. Soils* **2025**, *61*, 1183–1196. [CrossRef]
82. Wei, X.M.; Hu, Y.J.; Peng, P.Q.; Zhu, Z.K.; Atere, C.T.; O'Donnell, A.G.; Wu, J.H.; Ge, T.D. Effect of P stoichiometry on the abundance of nitrogen-cycle genes in phosphorus-limited paddy soil. *Biol. Fertil. Soils* **2017**, *53*, 767–776. [CrossRef]
83. Azzoni, R.; Giordani, C.; Bartoli, M.; Welsh, D.T.; Viaroli, P. Iron, sulphur and phosphorus cycling in the rhizosphere sediments of a eutrophic *Ruppia cirrhosa* meadow (Valle Smarlacca, Italy). *J. Sea Res.* **2001**, *45*, 15–26. [CrossRef]
84. Teng, Z.D.; Zhu, Y.Y.; Li, M.; Whelan, M.J. Microbial community composition and activity controls phosphorus transformation in rhizosphere soils of the Yeyahu Wetland in Beijing, China. *Sci. Total Environ.* **2018**, *628–629*, 1266–1277. [CrossRef] [PubMed]
85. Wei, T.; Liu, X.; Dong, M.F.; Lv, X.; Hua, L.; Jia, H.L.; Ren, X.H.; Yu, S.H.; Guo, J.K.; Li, Y.T. Rhizosphere iron and manganese-oxidizing bacteria stimulate root iron plaque formation and regulate Cd uptake of rice plants (*Oryza sativa* L.). *J. Environ. Manag.* **2021**, *278*, 111533. [CrossRef] [PubMed]
86. Babar, S.; Jilani, G.; Mihoub, A.; Jamal, A.; Ahmad, I.; Chaudhary, A.N.; Saeed, M.F.; Alam, T. Bacterial Redox Cycling of Manganese in Calcareous Soil Enhances the Nutrients Bioavailability to Wheat. *J. Soil Sci. Plant Nutr.* **2022**, *22*, 1215–1223. [CrossRef]
87. Brodersen, K.E.; Siboni, N.; Nielsen, D.A.; Pernice, M.; Ralph, P.J.; Seymour, J.; Kühl, M. Seagrass rhizosphere microenvironment alters plant-associated microbial community composition. *Environ. Microbiol.* **2018**, *20*, 2854–2864. [CrossRef] [PubMed]
88. Pfeffer, C.; Larsen, S.; Song, J.; Dong, M.; Besenbacher, F.; Meyer, R.L.; Kjeldsen, K.U.; Schreiber, L.; Gorby, Y.A.; El-Naggar, M.Y.; et al. Filamentous bacteria transport electrons over centimetre distances. *Nature* **2012**, *491*, 218–221. [CrossRef] [PubMed]
89. Scholz, V.V.; Martin, B.C.; Meyer, R.; Schramm, A.; Fraser, M.W.; Nielsen, L.P.; Kendrick, G.A.; Risgaard-Petersen, N.; Burdorf, L.D.W.; Marshall, I.P.G. Cable bacteria at oxygen-releasing roots of aquatic plants: A widespread and diverse plant–microbe association. *New Phytol.* **2021**, *232*, 2138–2151. [CrossRef] [PubMed]
90. Frenzel, P.; Rothfuss, F.; Conrad, R. Oxygen profiles and methane turnover in a flooded rice microcosm. *Biol. Fertil. Soils* **1992**, *14*, 84–89. [CrossRef]
91. Gilbert, B.; Frenzel, P. Rice roots and CH_4 oxidation: The activity of bacteria, their distribution and the microenvironment. *Soil Biol. Biochem.* **1998**, *30*, 1903–1916. [CrossRef]

92. Fritz, C.; Pancotto, V.A.; Elzenga, J.T.M.; Visser, E.J.W.; Grootjans, A.P.; Pol, A.; Iturraspe, R.; Roelofs, J.G.M.; Smolders, A.J.P. Zero methane emission bogs: Extreme rhizosphere oxygenation by cushion plants in Patagonia. *New Phytol.* **2011**, *190*, 398–408. [CrossRef] [PubMed]
93. Le Mer, J.; Roger, P. Production, oxidation, emission and consumption of methane by soils: A review. *Eur. J. Soil Biol.* **2001**, *37*, 25–50. [CrossRef]
94. Conrad, R. Soil microorganisms as controllers of atmospheric trace gases (H-2, CO, CH_4, OCS, N_2O, and NO). *Microbiol. Rev.* **1996**, *60*, 609–640. [CrossRef]
95. van Bodegom, P.; Stams, F.; Mollema, L.; Boeke, S.; Leffelaar, P. Methane oxidation and the competition for oxygen in the rice rhizosphere. *Appl. Environ. Microbiol.* **2001**, *67*, 3586–3597. [CrossRef] [PubMed]
96. Chen, Y.; Li, S.Y.; Zhang, Y.J.; Li, T.T.; Ge, H.M.; Xia, S.M.; Gu, J.F.; Zhang, H.; Lü, B.; Wu, X.X.; et al. Rice root morphological and physiological traits interaction with rhizosphere soil and its effect on methane emissions in paddy fields. *Soil Biol. Biochem.* **2019**, *129*, 191–200. [CrossRef]
97. Waldo, N.B.; Hunt, B.K.; Fadely, E.C.; Moran, J.J.; Neumann, R.B. Plant root exudates increase methane emissions through direct and indirect pathways. *Biogeochemistry* **2019**, *145*, 213–234. [CrossRef]
98. Määttä, T.; Malhotra, A. The hidden roots of wetland methane emissions. *Glob. Change Biol.* **2024**, *30*, e17127. [CrossRef] [PubMed]
99. Wang, J.X.; Man, Y.; Ruan, W.F.; Tam, N.F.Y.; Tao, R.; Yin, L.; Yang, Y.; Dai, Y.; Tai, Y.P. The effect of rhizosphere and the plant species on the degradation of sulfonamides in model constructed wetlands treating synthetic domestic wastewater. *Chemosphere* **2022**, *288*, 132487. [CrossRef] [PubMed]
100. Liu, X.; Chu, L.G.; Chen, H.Y.; Williams, P.N.; Sun, H.T.; Wang, B.Y.; Li, X.T.; Wang, L.Y.; Yu, H.R.; Zhang, S.L.; et al. Root-Driven Reactive Oxygen Species Controls Multidimensional Arsenic Speciation in the Rice Rhizosphere. *Environ. Sci. Technol.* **2026**, *60*, 12953–12964. [CrossRef] [PubMed]
101. Wu, B.; Wang, J.; Dai, H.; Yuan, H.; Ma, J.; Yu, W.; Zheng, X.; Ma, B.; Chen, B.; Chu, C. Radial oxygen loss triggers diel fluctuation of cadmium dissolution in the rhizosphere of rice. *Environ. Sci. Technol.* **2024**, *58*, 14718–14725. [CrossRef] [PubMed]
102. Das, S.; Chou, M.L.; Jean, J.S.; Liu, C.C.; Yang, H.J. Water management impacts on arsenic behavior and rhizosphere bacterial communities and activities in a rice agro-ecosystem. *Sci. Total Environ.* **2016**, *542*, 642–652. [CrossRef] [PubMed]
103. Li, S.S.; Chen, S.B.; Wang, M.; Lei, X.Q.; Zheng, H.; Sun, X.Y.; Wang, L.F.; Han, Y. Iron fractions responsible for the variation of Cd bioavailability in paddy soil under variable pe+pH conditions. *Chemosphere* **2020**, *251*, 126355. [CrossRef] [PubMed]
104. Wang, G.L.; Chi, T.Y.; Li, R.X.; Li, T.; Zhang, X.L. Harnessing the rhizosphere sponge to smooth pH fluctuations and stabilize contaminant retention in biofiltration system. *Bioresour. Technol.* **2025**, *418*, 131971. [CrossRef] [PubMed]
105. Xu, Y.G.; Feng, J.Y.; Li, H.S. Water management increased rhizosphere redox potential and decreased Cd uptake in a low-Cd rice cultivar but decreased redox potential and increased Cd uptake in a high-Cd rice cultivar under intercropping. *Sci. Total Environ.* **2021**, *751*, 141701. [CrossRef] [PubMed]
106. Hansel, C.M.; Fendorf, S.; Sutton, S.; Newville, M. Characterization of Fe plaque and associated metals on the roots of mine-waste impacted aquatic plants. *Environ. Sci. Technol.* **2001**, *35*, 3863–3868. [CrossRef] [PubMed]
107. Wang, X.; Ye, Z.H.; Li, B.; Huang, L.N.; Meng, M.; Shi, J.B.; Jiang, G.B. Growing Rice Aerobically Markedly Decreases Mercury Accumulation by Reducing Both Hg Bioavailability and the Production of MeHg. *Environ. Sci. Technol.* **2014**, *48*, 1878–1885. [CrossRef] [PubMed]
108. Dong, M.F.; Feng, R.W.; Wang, R.G.; Sun, Y.; Ding, Y.Z.; Xu, Y.M.; Fan, Z.L.; Guo, J.K. Inoculation of Fe/Mn-oxidizing bacteria enhances Fe/Mn plaque formation and reduces Cd and As accumulation in Rice Plant tissues. *Plant Soil* **2016**, *404*, 75–83. [CrossRef]
109. Passatore, L.; Rossetti, S.; Juwarkar, A.A.; Massacci, A. Phytoremediation and bioremediation of polychlorinated biphenyls (PCBs): State of knowledge and research perspectives. *J. Hazard. Mater.* **2014**, *278*, 189–202. [CrossRef] [PubMed]
110. Shimp, J.F.; Tracy, J.C.; Davis, L.C.; Lee, E.; Huang, W.; Erickson, L.E.; Schnoor, J.L. Beneficial effects of plants in the remediation of soil and groundwater contaminated with organic materials. *Crit. Rev. Environ. Sci. Technol.* **1993**, *23*, 41–77. [CrossRef]
111. Williams, J.B. Phytoremediation in wetland ecosystems: Progress, problems, and potential. *Crit. Rev. Plant Sci.* **2002**, *21*, 607–635. [CrossRef]
112. Yan, Z.S.; Jiang, H.L.; Cai, H.Y.; Zhou, Y.L.; Krumholz, L.R. Complex Interactions Between the Macrophyte *Acorus calamus* and Microbial Fuel Cells During Pyrene and Benzo[a]Pyrene Degradation in Sediments. *Sci. Rep.* **2015**, *5*, 10709. [CrossRef] [PubMed]
113. Gribsholt, B.; Kostka, J.E.; Kristensen, E. Impact of fiddler crabs and plant roots on sediment biogeochemistry in a Georgia saltmarsh. *Mar. Ecol.-Prog. Ser.* **2003**, *259*, 237–251. [CrossRef]
114. Kreuzwieser, J.; Buchholz, J.; Rennenberg, H. Emission of methane and nitrous oxide by Australian mangrove ecosystems. *Plant Biol.* **2003**, *5*, 423–431. [CrossRef]

115. Pedersen, O.; Binzer, T.; Borum, J. Sulphide intrusion in eelgrass (*Zostera marina* L.). *Plant Cell Environ.* **2004**, *27*, 595–602. [CrossRef]
116. Timmers, R.A.; Strik, D.P.B.T.B.; Hamelers, H.V.M.; Buisman, C.J.N. Long-term performance of a plant microbial fuel cell with *Spartina anglica*. *Appl. Microbiol. Biotechnol.* **2010**, *86*, 973–981. [CrossRef] [PubMed]
117. Chen, Z.; Huang, Y.C.; Liang, J.H.; Zhao, F.; Zhu, Y.G. A novel sediment microbial fuel cell with a biocathode in the rice rhizosphere. *Bioresour. Technol.* **2012**, *108*, 55–59. [CrossRef] [PubMed]
118. Ahkami, A.H.; Qafoku, O.; Roose, T.; Mou, Q.; Lu, Y.; Cardon, Z.G.; Wu, Y.; Chou, C.; Fisher, J.B.; Varga, T.; et al. Emerging sensing, imaging, and computational technologies to scale nano-to macroscale rhizosphere dynamics: Review and research perspectives. *Soil Biol. Biochem.* **2024**, *189*, 109253. [CrossRef] [PubMed]
119. Limmer, M.A.; Evans, A.E.; Seyfferth, A.L. A New Method to Capture the Spatial and Temporal Heterogeneity of Aquatic Plant Iron Root Plaque In Situ. *Environ. Sci. Technol.* **2021**, *55*, 912–918. [CrossRef] [PubMed]
120. Revsbech, N.P.; Pedersen, O.; Reichardt, W.; Briones, A. Microsensor analysis of oxygen and pH in the rice rhizosphere under field and laboratory conditions. *Biol. Fertil. Soils* **1999**, *29*, 379–385. [CrossRef]
121. Bezbaruah, A.N.; Zhang, T.C. pH, redox, and oxygen microprofiles in rhizosphere of bulrush (*Scirpus validus*) in a constructed wetland treating municipal wastewater. *Biotechnol. Bioeng.* **2004**, *88*, 60–70. [CrossRef] [PubMed]
122. Tschiersch, H.; Liebsch, G.; Borisjuk, L.; Stangelmayer, A.; Rolletschek, H. An imaging method for oxygen distribution, respiration and photosynthesis at a microscopic level of resolution. *New Phytol.* **2012**, *196*, 926–936. [CrossRef] [PubMed]
123. Santner, J.; Larsen, M.; Kreuzeder, A.; Glud, R.N. Two decades of chemical imaging of solutes in sediments and soils: A review. *Anal. Chim. Acta* **2015**, *878*, 9–42. [CrossRef] [PubMed]
124. Blossfeld, S.; Gansert, D.; Thiele, B.; Kuhn, A.J.; Lösch, R. The dynamics of oxygen concentration, pH value, and organic acids in the rhizosphere of *Juncus* spp. *Soil Biol. Biochem.* **2011**, *43*, 1186–1197. [CrossRef]
125. Brodersen, K.E.; Koren, K.; Lichtenberg, M.; Kühl, M. Nanoparticle-based measurements of pH and O_2 dynamics in the rhizosphere of *Zostera marina* L.: Effects of temperature elevation and light-dark transitions. *Plant Cell Environ.* **2016**, *39*, 1619–1630. [CrossRef] [PubMed]
126. Dai, H.Y.; Wu, B.B.; Chen, B.L.; Ma, B.; Chu, C.H. Diel Fluctuation of Extracellular Reactive Oxygen Species Production in the Rhizosphere of Rice. *Environ. Sci. Technol.* **2022**, *56*, 9075–9082. [CrossRef] [PubMed]
127. Callahan, B.J.; McMurdie, P.J.; Rosen, M.J.; Han, A.W.; Johnson, A.J.A.; Holmes, S.P. DADA2: High-resolution sample inference from Illumina amplicon data. *Nat. Methods* **2016**, *13*, 581–583. [CrossRef] [PubMed]
128. Srivastava, A.; Akhter, Y.; Verma, D. A step-by-step procedure for analysing the 16S rRNA-based microbiome diversity using QIIME 2 and comprehensive PICRUSt2 illustration for functional prediction. *Arch. Microbiol.* **2024**, *206*, 467. [CrossRef] [PubMed]
129. Radajewski, S.; Ineson, P.; Parekh, N.R.; Murrell, J.C. Stable-isotope probing as a tool in microbial ecology. *Nature* **2000**, *403*, 646–649. [CrossRef] [PubMed]
130. Wang, S.; Shan, J.; Xia, Y.; Tang, Q.; Xia, L.; Lin, J.; Yan, X. Different effects of biochar and a nitrification inhibitor application on paddy soil denitrification: A field experiment over two consecutive rice-growing seasons. *Sci. Total Environ.* **2017**, *593–594*, 347–356. [CrossRef] [PubMed]
131. Yuan, D.; Wu, S.; Hu, C.; Tang, J.; Qin, S. Biochar's electron shuttle potential mitigates N_2O emissions by counteracting the stimulatory effect of rice root iron plaque. *Geoderma* **2025**, *456*, 117248. [CrossRef]
132. Cayuela, M.L.; van Zwieten, L.; Singh, B.P.; Jeffery, S.; Roig, A.; Sánchez-Monedero, M.A. Biochar's role in mitigating soil nitrous oxide emissions: A review and meta-analysis. *Agric. Ecosyst. Environ.* **2014**, *191*, 5–16. [CrossRef]

Disclaimer/Publisher's Note: The statements, opinions and data contained in all publications are solely those of the individual author(s) and contributor(s) and not of MDPI and/or the editor(s). MDPI and/or the editor(s) disclaim responsibility for any injury to people or property resulting from any ideas, methods, instructions or products referred to in the content.